UNIVERSIDADE ESTADUAL DE CAMPINAS

FACULDADE DE ODONTOLOGIA DE PIRACICABA

GABRIELA ALVES DE CERQUEIRA

AVALIAÇÃO DE DIFERENTES CONCENTRAÇÕES DO FOSFATO DE CÁLCIO AMORFO E FLUORETO DE ESTANHO SOBRE AS PROPRIEDADES FÍSICO-QUÍMICAS DE UM INFILTRANTE RESINOSO EXPERIMENTAL

EVALUATION OF DIFFERENT CONCENTRATIONS OF AMORPHOUS CALCIUM PHOSPHATE AND STANNOUS FLUORIDE ON THE PHYSICOCHEMICAL PROPERTIES OF AN EXPERIMENTAL RESIN INFILTRANT

PIRACICABA

2024

GABRIELA ALVES DE CERQUEIRA

AVALIAÇÃO DE DIFERENTES CONCENTRAÇÕES DO FOSFATO DE CÁLCIO AMORFO E FLUORETO DE ESTANHO SOBRE AS PROPRIEDADES FÍSICO-QUÍMICAS DE UM INFILTRANTE RESINOSO EXPERIMENTAL

EVALUATION OF DIFFERENT CONCENTRATIONS OF AMORPHOUS CALCIUM PHOSPHATE AND STANNOUS FLUORIDE ON THE PHYSICOCHEMICAL PROPERTIES OF AN EXPERIMENTAL RESIN INFILTRANT

Tese apresentada à Faculdade de Odontologia de Piracicaba da Universidade Estadual de Campinas como parte dos requisitos exigidos para a obtenção do título de Doutora em Clínica Odontológica, na Área de Dentística.

Thesis presented to the Piracicaba Dental School of the University of Campinas in partial fulfillment of the requirements for the degree of Doctor in Clinical Dentistry, in Restorative Dentistry area.

Orientadora: Profª Drª Giselle Maria Marchi

ESTE EXEMPLAR CORRESPONDE À VERSÃO FINAL DA TESE DEFENDIDA PELA ALUNA GABRIELA ALVES DE CERQUEIRA E ORIENTADA PELA PROF. DRA. GISELLE MARIA MARCHI.

Piracicaba
2024

Ficha catalográfica
Universidade Estadual de Campinas (UNICAMP)
Biblioteca da Faculdade de Odontologia de Piracicaba
Marilene Girello - CRB 8/6159

C335a

Cerqueira, Gabriela Alves de, 1993-
Avaliação de diferentes concentrações do fosfato de cálcio amorfo e fluoreto de estanho sobre as propriedades físico-químicas de um infiltrante resinoso experimental / Gabriela Alves de Cerqueira. – Piracicaba, SP : [s.n.], 2024.

Orientador: Giselle Maria Marchi.
Tese (doutorado) – Universidade Estadual de Campinas (UNICAMP), Faculdade de Odontologia de Piracicaba.

1. Cárie dentária. 2. Infiltração resinosa. 3. Fosfato de cálcio amorfo. 4. Remineralização dentária. 5. Fluoretos de estanho. I. Marchi, Giselle Maria, 1970-. II. Universidade Estadual de Campinas (UNICAMP). Faculdade de Odontologia de Piracicaba. III. Título.

Informações Complementares

Título em outro idioma: Evaluation of different concentrations of amorphous calcium phosphate and stannous fluoride on the physicochemical properties of an experimental resin infiltrant
Palavras-chave em inglês:
Dental caries
Resin infiltration
Amorphous calcium phosphate
Tooth remineralization
Tin fluorides
Área de concentração: Dentística
Titulação: Doutora em Clínica Odontológica
Banca examinadora:
Giselle Maria Marchi [Orientador]
Paula Mathias Rabelo de Morais
Larissa Sgarbosa de Araújo Matuda
Carolina Steiner Oliveira Alarcon
Waldemir Francisco Vieira Junior
Data de defesa: 11-06-2024
Programa de Pós-Graduação: Clínica Odontológica

Identificação e informações acadêmicas do(a) aluno(a)
- ORCID do autor: https://orcid.org/0000-0002-4581-6797
- Currículo Lattes do autor: http://lattes.cnpq.br/5493479310712612

UNIVERSIDADE ESTADUAL DE CAMPINAS
Faculdade de Odontologia de Piracicaba

A Comissão Julgadora dos trabalhos de Defesa de Tese de Doutorado, em sessão pública realizada em 11 de junho de 2024, considerou a candidata GABRIELA ALVES DE CERQUEIRA aprovada.

PROFª. DRª. GISELLE MARIA MARCHI

PROFª. DRª. PAULA MATHIAS RABELO DE MORAIS

PROFª. DRª. LARISSA SGARBOSA DE ARAÚJO MATUDA

PROFª. DRª. CAROLINA STEINER OLIVEIRA ALARCON

PROF. DR. WALDEMIR FRANCISCO VIEIRA JUNIOR

A Ata da defesa, assinada pelos membros da Comissão Examinadora, consta no SIGA/Sistema de Fluxo de Dissertação/Tese e na Secretaria do Programa da Unidade.

DEDICATÓRIA

Dedico este trabalho à minha mãe Neide e ao meu pai Eduardo (in memoriam), por todos os ensinamentos passados, por todas as horas de cuidado e atenção, por todo amor, apoio e compreensão desde o meu nascimento. Painho, olha só onde eu cheguei!! Obrigada mãe, obrigada pai, por todas as horas de “dever de casa” que fizemos juntos. Obrigada por me ensinarem a ser forte, responsável, dedicada e perseverante. Essa conquista é nossa e, eu amo vocês com todo o meu coração!

AGRADECIMENTOS

Este trabalho foi realizado com apoio da Coordenação de Aperfeiçoamento de Pessoal de Nível Superior – Brasil (CAPES) – Código de financiamento 001.

À **Deus** e todas as suas dádivas. Muito obrigada, meu senhor, por me proteger, me sustentar e me guiar até aqui.

À Universidade Estadual de Campinas (UNICAMP), na pessoa do Magnífico Reitor, Prof. Dr. Antônio José de Almeida Meirelles e da coordenadora geral da Universidade Profa. Dra. Maria Luiza Moretti.

À direção da Faculdade de Odontologia de Piracicaba da Universidade Estadual de Campinas, na pessoa do Diretor Prof. Dr. Flávio Henrique Baggio Aguiar e da Diretora Associada Profa. Dra. Karina Gonzales Silvério Ruiz.

Aos Professores da Área de Dentística, Profa. Dra. Giselle Maria Marchi, Profa. Dra. Débora Alves Nunes Leite Lima, Prof. Dr. Flávio H. Baggio Aguiar, Prof. Dr. Luís Roberto M. Martins, Profa. Dra. Vanessa Cavalli Gobbo, Prof. Dr. Waldemir Francisco Vieira Júnior e Prof. Dr. Marcelo Giannini, por todo conhecimento compartilhado ao longo da trajetória.

À minha orientadora, Profª. Drª. **Giselle Maria Marchi**, sempre muito humana, gentil e compreensível. Obrigada, professora Giselle, por ter sido calmaria em muitos momentos de tensão e por todo o auxílio, acolhimento e carinho de sempre nesta trajetória.

À toda minha **família**, em especial à minha **mãe** e minha **irmã**, por todo suporte, compreensão e torcida de sempre. Vocês foram essenciais nesse longo caminhar!!

Ao meu namorado e grande parceiro **Guilherme Gambin** por toda ajuda, por ser escuta ativa e tranquilidade nos momentos de tensão, por todo acolhimento e amor de sempre.

Aos meus **colegas e amigos da Pós-graduação e da vida**, pela vivência, troca de conhecimento e leveza. Em especial à **Isadora Rodrigues,** que contribuiu demais com este trabalho, e se fez uma grande amiga para a vida. Muito obrigada pela parceria, Isa!

À minha **banca avaliadora** de qualificação e defesa pela disponibilidade, atenção e cuidado para com este trabalho.

“ Faça o teu melhor na condição que você tem, enquanto você não tem condições melhores para fazer melhor ainda.”

Mário Sergio Cortella

RESUMO

Materiais bioativos têm apresentado relevante importante na Odontologia, considerando sua efetividade no controle das lesões de cárie, por meio de trocas iônicas com o meio bucal. Este estudo avaliou a influência da incorporação de diferentes concentrações (0%, 1%, 1,5% e 2%) de fosfato de cálcio amorfo (ACP) e fluoreto de estanho (SnF2) nas propriedades físico-químicas de grau de conversão, ângulo de contato, sorção e solubilidade, profundidade de penetração, liberação iônica, estabilidade de cor e rugosidade de um infiltrante experimental, comparado ao controle comercial. Os grupos avaliados foram: controle comercial (Icon), controle experimental (98,5% blend TEGDMA-BisEMA; 0.5% CQ; 1% EDAB), 1ACP, 1.5ACP, 2ACP, 1SnF2, 1.5SnF2 e 2SnF2. Para o grau de conversão (n=5) foi utilizado um espectrômetro de raios infravermelhos transformado de Fourier (FTIR-ATR). Para o ângulo de contato (n=16) foi utilizado um goniômetro. Para os testes de sorção e solubilidade (n=16), as amostras foram pesadas em períodos de desidatração e hidratação. Para a análise da profundidade de penetração (n=5), amostras de dente com lesão de cárie incipiente foram coradas, infiltradas, cortadas em fatias, polidas e levadas ao microscópio confocal de varredura a laser. Para liberação iônica (n=3), amostras de infiltrantes foram imersas em uma solução tamponada (pH 4) e, as concentrações dos íons Ca, P e F foram medidas nos intervalos de 14 e 28 dias por um espectrofotometro de absorbância. Para a estabilidade de cor (n=15) e rugosidade superficial (n=15), amostras de dente com lesão de cárie incipiente foram infiltradas, imersas em solução de café e polidas após o manchamento. As leituras de estabilidade de cor e rugosidade foram realizadas para o (I) esmalte infiltrado, (II) esmalte manchado e (III) esmalte polido. A análise dos dados foi realizada utilizando o software R, com nível de significância de 5%. O grupo controle experimental teve o maior grau de conversão. Os grupos controles experimental e comercial apresentaram menor ângulo de contato e menor sorção e solubilidade. Todos os grupos apresentaram penetração no esmalte desmineralizado, exceto o 2SnF2. Todos os grupos com partícula foram estatisticamente iguais na liberação dos íons Ca e P. O grupo 2Snf2 apresentou liberação de íons F em 14 dias. Os grupos com SnF2 tiveram maior variação de cor após manchamento. Todos os grupos com partícula tiveram maior pigmentação do que os grupos controles. Todos os grupos tiveram redução do escurecimento após polimento. Todos os grupos com SnF2 apresentaram maior luminosidade após polimento. A rugosidade foi menor para todos os grupos no esmalte polido. Apesar de uma menor estabilidade de cor, a incorporação das partículas no infiltrante experimental não afetou negativamente as demais propriedades testadas, além de ter havido liberaçãao de íons F; o polimento foi capaz de reduzir a rugosidade e pigmentação dos grupos avaliados.

Palavras chaves: Cárie Dentária, Infiltração Resinosa, Remineralização Dentária, Fosfato de Cálcio Amorfo, Fluoreto de Estanho.

ABSTRACT

Bioactive materials have played an important role in dentistry, considering their effectiveness in controlling caries lesions through ionic exchange with the oral environment. This study evaluated the influence of incorporating different concentrations (0%, 1%, 1.5% and 2%) of amorphous calcium phosphate (ACP) and tin fluoride (SnF2) on the physicochemical properties of degree of conversion, contact angle, sorption and solubility, depth of penetration, ionic release, color stability and roughness of an experimental infiltrant, compared to the commercial control. The groups evaluated were: commercial control (Icon), experimental control (98.5% TEGDMA-BisEMA blend; 0.5% CQ; 1% EDAB), 1ACP, 1.5ACP, 2ACP, 1SnF2, 1.5SnF2 and 2SnF2. A Fourier transform infrared spectrometer (FTIR-ATR) was used to measure the degree of conversion (n=5). A goniometer was used for the contact angle (n=16). For the sorption and solubility tests (n=16), the samples were weighed during the dehydration and hydration periods. For the analysis of penetration depth (n=5), tooth samples with incipient caries lesions were stained, infiltrated, cut into slices, polished and taken to the laser scanning confocal microscope. For ion release (n=3), infiltrant samples were immersed in a buffered solution (pH 4) and the concentrations of Ca, P and F ions were measured at 14- and 28-day intervals using an absorbance spectrophotometer. For color stability (n=15) and surface roughness (n=15), tooth samples with incipient caries lesions were infiltrated, immersed in coffee solution and polished after staining. Color stability and roughness readings were taken for (I) infiltrated enamel, (II) stained enamel and (III) polished enamel. The data was analyzed using R software, with a significance level of 5%. The experimental control group had the highest degree of conversion. The experimental and commercial control groups had lower contact angles and lower sorption and solubility. All the groups penetrated demineralized enamel, except for 2SnF2. All particle groups were statistically equal in the release of Ca and P ions. The 2Snf2 group showed release of F ions within 14 days. The SnF2 groups had greater color variation after staining. All the particle groups had greater pigmentation than the control groups. All groups had reduced darkening after polishing. All groups with SnF2 had greater luminosity after polishing. Roughness was lower for all groups on polished enamel. Despite the lower color stability, the incorporation of the particles into the experimental infiltrant did not negatively affect the other properties tested, in addition to the release of F ions; polishing was able to reduce the roughness and pigmentation of the groups evaluated.

Keywords: Dental Caries, Resin Infiltration, Tooth Remineralization, Amorphous Calcium Phosphate, Stannous Fluoride.

SUMÁRIO

1 INTRODUÇÃO

A cárie dentária é considerada uma doença multifatorial por envolver interações entre o dente, o biofilme que se acumula sobre a estrutura dentária e açúcares provenientes da dieta; sofre, além disso, influências genéticas e salivares (Pitts et al., 2017). O processo carioso se forma a partir da alternância de períodos de desmineralização e remineralização, onde o avanço desse processo está diretamente relacionado à predominância da desmineralização, formando as lesões incipientes (Pitts et al., 2017), também conhecidas por lesão de mancha branca, considerada o primeiro sinal desta doença (De Rooij e Nancollas, 1984, Skucha-Nowak et al., 2016, Urquhart et al., 2019). Tais lesões são caracterizadas como lesões subsuperficiais, podendo apresentar dissolução dos minerais até o terço externo da dentina, apesar da manutenção da camada externa do esmalte, que se apresenta esbranquiçada, porosa e opaca (Phark et al., 2009).

As lesões de cárie incipientes recebem, normalmente, terapia de remineralização, envolvendo fontes de flúor, além da necessidade de mudanças comportamentais na dieta, por exemplo, visando assim a paralisação da progressão e/ou reversão da desmineralização do dente (Pitts et al., 2017, Lasfargues et al., 2013). Contudo, tal tratamento exige, na grande maioria da vezes, múltiplas sessões clínicas e grande cooperação do paciente como, comparecimento às consultas e controle adequado da higiene bucal e dieta; o que, por muitas vezes, é difícil de se obter (Lasfargues et al., 2013). Outro ponto a ser considerado é que, diante da não cooperação do paciente, um aumento da profundidade da lesão pode ocorrer, o que se faz pensar que tal tratamento, isoladamente, pode não ser eficaz para interromper a lesão cariosa e, a subsequente fragilização da superfície pode ocorrer, causando cavitação (Askar et al., 2018, Mandava et al., 2017). É muito comum, por exemplo, o surgimento de lesões de cárie incipientes nas faces proximais dos dentes, sendo, por muitas vezes, o tratamento convencional utilizado, nesses casos, a remoção da lesão de cárie e preenchimento com resina composta, às custas da destruição de uma quantidade substancial de estrutura dental sadia em prol da obtenção de acesso à lesão (Askar et al., 2018).

Diante dessas considerações e do avanço da Odontologia Minimamente Invasiva, foi então desenvolvida a técnica infiltrativa com um agente resinoso fotopolimerizável denominado infiltrante, a fim de prevenir a progressão da lesão de cárie incipiente (Lasfargues et al., 2013, Golz et al., 2016). Tal técnica tem como principal indicação lesões de cárie incipientes até o terço externo da dentina (não cavitadas), presentes em superfícies

lisas de dentes decíduos e permanentes (Lasfargues et al., 2013). Seu mecanismo de ação se dá pela penetração do material resinoso nos poros do esmalte, através de forças capilares, bloqueando as vias de difusão de ácidos cariogênicos e minerais dissolvidos, contribuindo para a paralisação da progressão da lesão cariosa, após sua fotopolimerização (Lasfargues et al., 2013, Askar et al., 2018, Abbas et al., 2018). Ou seja, as bactérias que habitam no esmalte desmineralizado ficam presas na resina infiltrada (Paris et al., 2010). Tal material resinoso tem oferecido vantagens como estabilização mecânica do esmalte desmineralizado, preservação da estrutura dental sadia, minimização do risco de lesões de cárie secundárias, retardo da intervenção restauradora invasiva, baixo ou nenhum risco de sensibilidade pós-operatória e inflamação pulpar, redução do risco de gengivite e boa aceitação pelo paciente em relação à técnica aplicada (Prajapati et al., 2017).

O infiltrante resinoso Icon®, único disponível comercialmente, é um material de baixa viscosidade e alto coeficiente de penetração, constituído por uma matriz resinosa à base de TEGDMA, iniciadores e aditivos (Lasfargues et al., 2013, Golz et al., 2016). Entretanto, apesar de estudos prévios demonstrarem resultados promissores sobre a eficácia do infiltrante Icon® (Paris et al., 2010, Ekstrand et al., 2010, Golz et al., 2016), novas formulações de infiltrantes resinosos experimentais têm sido estudadas, objetivando aprimorar as características e o desempenho do material, de acordo com o objetivo do tratamento. Um material com alta concentração de TEGDMA pode apresentar alta degradação hidrolítica em meio oral e maior contração de polimerização devido ao seu baixo peso molecular, apesar da alta fluidez e boa profundidade de penetração (Sideridou et al., 2002). Assim, formulações experimentais têm sido sugeridas, sendo uma dessas à base de 25% BisEMA, 75% TEGDMA, 0,5% de Canforoquinona e 1% de Etil 4-dimetilamino benzoato (EDMAB), estudada por Ganglianone et al. (2020), apresentando resultados favoráveis em relação, por exemplo, quanto ao grau de conversão e sorção e solubilidade; sendo também comprovados nos estudos de Mathias et al. (2019) e Pedreira et al. (2021).

Somado a isso e, acreditando no efeito terapêutico do infiltrante resinoso, tem-se sugerido a adição de partículas bioativas ao material resinoso, a fim de se observar o efeito remineralizante que este material pode proporcionar às lesões de cárie incipientes (Par et al., 2018, Sfalcin et al., 2017). Sabe-se que os componentes da saliva como o flúor, cálcio e fosfato biodisponíveis contribuem para a formação da fluorapatita (Fernando et al., 2019); porém, em determinados casos, a saliva pode apresentar limitação de ação remineralizante, especialmente em pacientes que apresentam dieta muito rica em carboidratos, com higiene bucal deficiente, além daqueles com algum distúrbio sistêmico e/ou sob uso de

medicamentos cujo um dos efeitos colaterais é a hipossalivação (Fernando et al., 2019). Pensando nisso, tem-se sugerido em agentes que forneçam íons de cálcio e fosfato para a remineralização do dente desmineralizado, como por exemplo o Fosfato de Cálcio Amorfo (ACP) .

O ACP é apresentado como um pó branco, cujas partículas apresentam tamanho <150 nanômetros. Sendo considerado um biomimético salivar que fornece íons de cálcio e de fosfato, a fim de inibir a desmineralização e promover a remineralização das lesões de mancha branca (Cross et al., 2007, Cochrane et al., 2008, Fernando et al., 2019). Além disso, considerando que o infiltrante resinoso tem em sua composição monômeros passíveis de uma maior contração de polimerização, como o TEGDMA, a adição de partículas bioativas como o ACP pode promover a remineralização de áreas do esmalte onde, por ventura, não houver preenchimento adequado com o material resinoso, a partir da liberação de íons cálcio e fosfato, reduzindo as chances de progressão das lesões e, lesões de cárie secundária (Fernando et al., 2019, Zixiang et al., 2022). Estudos anteriores exibiram resultados promissores sobre a incorporação de 10 a 30% das partículas de ACP em materiais resinosos, como o infiltrante resinoso e um adesivo (Gao et al., 2020, Fan et al., 2021, Zixiang et al., 2022).

Além do ACP, o fluoreto de estanho (SnF2) tem demonstrado, em estudos prévios, tanto pelos íons de estanho quanto pelos íons fluoretos, eficácia na inibição da desmineralização do esmalte provocada por ácidos diversos (Schlueter et al., 2009, Ganss et al., 2010). O SnF2, apresentado em forma de pó cristalizado (granuloso), é considerado um composto fluoretado polivalente com cátions metálicos (Sn^{2+}) (Schlueter et al., 2009) e, seu mecanismo de ação é baseado, especialmente, na reação do estanho com o tecido dental, formando assim precipitados ricos em metais, além dos sais de fluoreto de cálcio (CaF_2) (Babcock et al., 1978). Acredita-se que o estanho possa interagir com a superfície do dente e, além disso, exercer papel preventivo em relação à exposição do cálcio, presente no esmalte dental, aumentando também sua resistência à desmineralização, frente aos desafios ácidos presentes no ambiente oral (Faller e Eversole, 2014, Cheng et al., 2017); ou seja, diante de períodos de desmineralização e re-deposição mineral, o estanho pode ser incorporado ao substrato dental desmineralizado, formando áreas estruturalmente modificadas e menos solúveis a tais desafios ácidos (Schlueter et al., 2009).

Sabe-se que o infiltrante resinoso vem sendo considerado um tratamento alternativo aos tratamentos não invasivos e invasivos já consagrados na Odontologia, eliminando as implicações e limitações já reconhecidas. Infere-se assim que a adição das partículas de ACP e

SnF2 ao infiltrante resinoso pode proporcionar ao material um efeito remineralizante, elevando seu desempenho, além de exercer papel protetor frente aos novos períodos de desmineralização, inerentes ao ambiente bucal. E, apesar de saber da eficácia do infiltrante resinoso e das partículas (Peters et al., 2019, Paris et al., 2020, Yanwei et al., 2021, Konradsson et al., 2020), isoladamente, ainda há poucos estudos sobre o comportamento e efeito terapêutico de um infiltrante resinoso preenchido com partículas bioativas. Portanto, este estudo teve como objetivo avaliar a influência da incorporação de diferentes concentrações (0%, 1%, 1,5% e 2%) de partículas de ACP e SnF2 nas propriedades de grau de conversão, ângulo de contato, sorção e solubilidade, profundidade de penetração, liberação iônica, estabilidade de cor e rugosidade de um infiltrante experimental, comparado ao controle comercial. As hipóteses deste trabalho são as de que (I) haveria diferença entre os grupos nas propriedades físico-químicas testadas e (II) haveria diferença entre os tempos avaliados para rugosidade superficial.

2 ARTIGO: Physical-chemical properties of resin infiltrants containing different concentrations of amorphous calcium phosphate and stannous fluoride: in vitro study.

Artigo submetido ao periódico Clinical Oral Investigations (Anexo 3).

<Gabriela Alves **de Cerqueira**, Isadora Cezar **Rodrigues**, Jade Laísa Gordilio **Zago**, Flávio Henrique Baggio **Aguiar**, Giselle Maria **Marchi**>

Department of Restorative Dentistry, Piracicaba Dental School, University of Campinas, Piracicaba, São Paulo, 13414-903, Brazil.

Corresponding Author:

Gabriela Alves de Cerqueira

Department of Restorative Dentistry, Av. Limeira, 901, Piracicaba Dental School, University of Campinas, Piracicaba, São Paulo, 13414-903, Brazil. Phone: +55 (019) 2106-5341

Email: gabrielaac3@gmail.com

*Este trabalho foi realizado no formato alternativo conforme Deliberação da Congregação da Faculdade de Odontologia de Piracicaba No 306/2010 da Universidade Estadual de Campinas.

Physical-chemical properties of resin infiltrants containing different concentrations of amorphous calcium phosphate and stannous fluoride: in vitro study

ABSTRACT

Objective: To evaluate the influence of incorporating different concentrations (0%, 1%, 1.5% and 2%) of amorphous calcium phosphate (ACP) and tin fluoride (SnF2) on the degree of conversion (DC), contact angle (CA), water sorption (WS) and solubility (SL), penetration depth, ionic release, color stability and roughness of experimental resin infiltrants. **Methods and materials:** The groups evaluated were: commercial control (Icon), experimental control (98,5% wt blend TEGDMA-BisEMA; 0.5% wt CQ; 1% wt EDAB), 1ACP, 1.5ACP, 2ACP, 1SnF2, 1.5SnF2 and 2SnF2. A Fourier transform infrared spectrometer was used for DC (n=5). A goniometer was used for the contact angle (n=16). The samples were weighed during the dehydration and hydration periods for WS and SL (n=16). For the penetration depth (n=5), images were obtained using a confocal laser scanning microscope and analyzed qualitatively. The concentrations of Ca, P and F ions were measured at 14 and 28 days using a spectrophotometer (n=3). For color stability (n=15) and roughness (n=15), readings were taken at three different times: (I) infiltrated enamel, (II) stained enamel and (III) polished enamel. Data analysis was carried out using R software, with a significance level of 5%. **Results:** The experimental control group had the highest degree of conversion. The control groups had lower contact angles and lower sorption and solubility. All groups showed penetration into demineralized enamel, except for 2SnF2. The 2Snf2 group showed release of F- ions within 14 days. All the particle groups had greater pigmentation than the controls. All groups had reduced darkening after polishing. Roughness was lower for all groups on polished enamel. **Conclusions:** Despite lower color stability, the incorporation of the particles into the experimental infiltrant did not negatively affect the other properties tested. **Clinical Relevance:** Resin infiltrants with bioactive particles could offer, in addition to paralyzing the caries lesion and strengthening the enamel subsurface, a remineralizing action with the release of its ions.

Keywords: Dental Caries, Resin Infiltration, Tooth Remineralization, Amorphous Calcium Phosphate, Tin Fluoride.

INTRODUCTION

Caries is a common, multifactorial and chronic disease [1]. The diagnosis and treatment of incipient caries lesions should be carried out as soon as possible in order to avoid the progression and cavitation of these lesions, making non-invasive or minimally invasive interventions possible [1,2]. This way, the resin infiltrant has become a satisfactory and conservative treatment option; presented as a micro-invasive alternative, whose its main objective is to penetrate the porous body of white spot caries lesions and paralyze the carious lesion, it is indicated for incipient lesions in enamel and up to the outer third of dentin [2]. Because of the similarity of its refractive index to that of sound enamel and, consequently, improve the patient's dental aesthetics [1,2]. Demonstrating favorable results within Minimally Invasive Dentistry, the resin material is also capable of masking lesions [1].

The only commercially available resin infiltrant, known as Icon®, has shown positive results in previous studies, in terms of stopping caries lesions [3,4]; however, new resin infiltrant formulations have been developed with the aim of improving the resin material in terms of its physical properties, such as reducing shrinkage and water sorption and solubility [5]. Furthermore, the incorporation of bioactive particles has been encouraged, considering the possibility of formulating a material that is capable of releasing ions and assisting in the remineralization and/or strengthening of dental enamel in the face of the acidic challenges encountered in the oral environment [6,7,8]

Bioactive particles such as amorphous calcium phosphate (ACP) have been incorporated into the resin infiltrant [9]. The mechanism of ACP particles is to increase the bioavailability of calcium and phosphate, favoring precipitation on the tooth and dissolution in saliva, thus, contributing to the remineralization of affected enamel [10,11]. Similarly, fluoride is also recognized as a remineralizing agent. Its ions, when acting together with bioavailable calcium and phosphate, contribute to the formation of fluohydroxyapatite, making enamel more resistant to acids [12]. Tin fluoride (SnF2), one of the sources of fluoride, has gained prominence, considering that tin ions can interact with the tooth surface. increasing its resistance to demineralization by preventing calcium exposure [12]. New resin infiltrant formulations require different physical tests to assess their performance, in order to meet some of the specific requirements for resin materials when submitted to the oral environment [7,8]. Such as solid-state polymerization capacity, resistance to chemical factors, appropriate aesthetics, non-toxicity, as well as a certain hydrophilicity, low viscosity and a smaller contact angle, which helps the material to penetrate the enamel properly [13,14].

The resin infiltrant has a monomer-based composition, similar to composite resin, adhesives or cements [6], which undergo water sorption and solubility, generating degradation over time [15,16] and, consequently, increased roughness [5]. In addition, previous studies have observed that the resin infiltrant tends to stain severely when subjected to different staining solutions [6,17,18]. The incorporation of particles can even influence the color stability of resin materials [6], making it important to evaluate the new formulations developed. In addition, a resin material tends to undergo changes in roughness. especially when exposed to humidity. temperature differences and acidity, which are commonly present in the oral environment [5]. Increased roughness can lead to greater deterioration of the restorative material, pigmentation, accumulation of biofilm and, consequently, periodontal problems in the patient [19,20].

Taking into account all features possibly promoted by the resin infiltrant incorporated by ACP and SnF2, it is necessary to analyze wheter its perfomance would be satisfatory. New resin infiltrant formulations require physical-chemical tests to assess their properties, in order to meet some of requirements for restorative resin materials. Furthermore, the addition of bioactive agents to the composition of the infiltrating material may contribute to the remineralization of subsurface enamel. Thus, the aim of the study to evaluate the influence of incorporating different concentrations (0%, 1%, 1.5% and 2%) of ACP and SnF2 particles on the properties of degree of conversion, contact angle, sorption and solubility, depth of penetration, ionic release, color stability and roughness of an experimental infiltrant, compared to the commercial control. The hypotheses of this work are that (I) there will be a difference between the groups in the physica-lchemical properties tested and (II) there will be a difference between the times evaluated for surface roughness.

MATERIALS AND METHODS

Formulation of the resin infiltrants

The compositions of the resin infiltrants are shown in Table 1, all in percentage by weight. A precision balance (Shimadzu, Tokyo, Japan) was used to weigh the reagents under yellow light. Next, each container with the mixture of reagents was taken to the speed mixer (Hauschild, Farmington Hills, USA) under 3000 RPMs for 5 minutes to homogenize the components. At the end, the resin infiltrants were stored individually under refrigeration at 4 ºC. The particle concentrations were obtained in a previous pilot study, without altering the general characteristics of the material.

Table 1 - Description of the groups and composition of the resin infiltrants evaluated.

Groups	Composition of infiltrators
Icon (commercial control)	Icon® (70-95% wt TEGDMA, <2.5% wt CQ and additions)
Base Exp (experimental control)	98,5% wt blend TEGDMA-BisEMA; 0.5% wt CQ; 1% wt EDAB
1ACP	97,5% wt blend TEGDMA-BisEMA; 0.5% wt CQ; 1% wt EDAB; 1% wt ACP
1.5ACP	97% wt blend TEGDMA-BisEMA; 0.5% wt CQ; 1% wt EDAB; 1.5% wt ACP
2ACP	96,5% wt blend TEGDMA-BisEMA; 0.5% wt CQ; 1% wt EDAB; 2% wt ACP
1SnF2	97,5% wt blend TEGDMA-BisEMA; 0.5% wt CQ; 1% wt EDAB; 1% wt SnF2
1.5SnF2	97% wt blend TEGDMA-BisEMA; 0.5% wt CQ; 1% wt EDAB; 1.5% wt SnF2
2SnF2	96,5% wt blend TEGDMA-BisEMA; 0.5% wt CQ; 1% wt EDAB; 2% wt SnF2

Icon® according to the manufacturer (DMG, Hamburg, Germany) (LOT 261398). BisEMA - Bisphenol A polyethylene glycol dimethacrylate (Sigma Aldrich Brasil Ltda, Barueri, SP, Brazil). TEGDMA - Triethylene glycol dimethacrylate (Sigma Aldrich Brasil Ltda, Barueri, SP, Brazil). CQ – Camphorquinone (Sigma Aldrich Brasil Ltda, Barueri, SP, Brazil). EDAB - Ethyl 4-dimethylamino benzoate (Sigma Aldrich Brasil Ltda, Barueri, SP, Brazil). ACP - Amorphous calcium phosphate (Sigma Aldrich Brasil Ltda, Barueri, SP, Brazil) (<150nm) and SnF2 - PA tin fluoride (Êxodo Científica, Sumaré, SP, Brazil).

Degree of conversion (DC)

Fourier transform infrared spectroscopy with attenuated total reflectance (FTIR-ATR) (Vertex 70 spectrometer, Bruker, Billerica, MA, USA) was used for the DC (n=5). The first reading of the resin material, not yet light-cured, was taken by depositing about 1μL of the resin infiltrants on the device's crystal using a pipette, so that the drop remained in the focal center of the equipment's laser beam. A polyester strip was then placed on top of the micro drop of material to standardize the samples. The material was then light-cured using an LED light source (Valo, Ultradent, Indaiatuba, SP, Brazil) with a power density of 1000mW/cm2 for 40 seconds. A second reading was taken after 2 minutes of waiting. The Opus v.6 software (Bruker Optics) was used to calculate the degree of conversion (in%). The corresponding baseline was plotted and the absorbance value of the baseline was subtracted from the maximum absorbance value at the corresponding wavenumber; The wavelengths used to obtain the values were 1610 and 1637.

Contact angle (CA)

The contact angle measurements were taken on a polished glass slide, cleaned with absolute alcohol and dried in an oven at 37ºC for 24 hours, changing at each analysis. A goniometer with attached camera (Ramé-hart

- 500F1, Succasunna, USA) was used to measure the contact angle of the resin infiltrants, with drops (approximately 1μL) dispensed perpendicularly into the surface of the glass slide using a precision micro syringe. Images were obtained from 10 measurements per sample, at a time interval of 0.05 seconds and frame averaging of 60 frames/second. The images obtained were analyzed using drop shape analysis software (DROPimage Advanced). For each group (n=16), the average of the contact angles on each side of the drop was calculated in degrees.

Water sorption (So) and solubility (SL)

Disc-shaped (5mm x 1mm) specimens of the resin infiltrants (n=16) were made using a silicone matrix and polymerized using a Valo LED light (Valo, Ultradent, Indaiatuba, SP, Brazil) with a power density of 1000mW/cm2 for 40 seconds; they were then placed in a desiccator and stored in an oven at 37º C. The samples were weighed daily on an analytical balance (Shimadzu, Tokyo, Japan) at 24-hour intervals until a constant mass (m1) was obtained, with a variation of less than 0.002 mg. To calculate the volume (mm^3), each sample had its thickness and diameter measured using a digital caliper (Mitutoyo, Japan). The samples were then stored at 37ºC in closed eppendorfs containing 1.5 mL of distilled water. After seven days of storage, the eppendorfs were removed from the oven and left at room temperature for 30 minutes; the samples were then gently dried with absorbent paper and weighed again on an analytical balance to obtain m2. After this period, the samples were desiccated and weighed again daily until a new constant mass (m3) was obtained. Sorption and solubility values were calculated using two specific formulas (So= m2-m3/V and SL= m1-m3/V), out in accordance with the ISO 4049/2019 specification.

Ion release

For this analysis. a 133 mmol/L sodium chloride (NaCl) solution was prepared and buffered with 50 mmol/L lactic acid to pH 4 [9]. Resin infiltrant samples from each group (n=3), measuring 2x2x12 mm. were made by inserting the resin material into a silicone matrix. To standardize the samples, a polyester matrix was used over the silicone matrix with the resin infiltrant and a 40-second light-curing process was carried out on the surface and bottom of each sample, for a total of 80 seconds. Each sample was then immersed in 17 mL of the prepared solution and the concentrations of calcium (Ca), phosphorus (P) and fluoride (F) ions were measured at two different times (14 and 28 days). For each time, a 4 mL fraction of the solution was removed, stored in an eppendorf and replaced with a new one. The eppendorfs with the fractions of the solution were kept closed and refrigerated throughout the period. The concentrations of the ions released were quantified using a absorbance spectrophotometer (UV-Visible, Thermo Scientific, São Paulo, SP, Brazil). To obtain the averages, the calcium ions released were read using the single-point calcium arsenazo method, using the absorbance values of a standard solution, and the arithmetic mean of this standard was determined in duplicate. For phosphorus and fluoride ions, the linear standard curve method was used, with absorbance duplicated for each point of the standard.

Simulation of the incipient carious lesion

Sample preparation

After approval by the Research Ethics Committee (no. 654486.22.6.0000.5418) sound human molars were selected. The teeth were cleaned with a Robinson brush and pumice stone to remove residues and then stored in a 0.1% thymol solution. The roots were then sectioned using a metallographic cutter (Buehler LTD, Lake Bluff, IL, USA) and dispensed. Next, samples measuring 5x5x2mm were obtained from the buccal and palatal surfaces of the teeth. To standardize the surfaces, the samples were lightly flattened in a polishing machine (Arotec S/A Indústria e Comércio, Cotia, SP, Brazil) with 600 and 1200 grit sandpaper (Buehler) under constant refrigeration; they were then polished with felt discs and diamond solution (1 μm; Buehler) and then stored in eppendorfs and kept at 37ºC.

Induction of the incipient carious lesion

After obtaining the samples, surface microhardness averages were obtained by taking three readings on a microdurometer (HMV-2000; Shimadzu Corporation, Tokyo, Japan), 100 μm apart from the center of the surface, to randomize the samples, to prevent groups from benefiting or suffering from low or high microhardness. Afterwards, the samples were protected with nail varnish (Colorama®, São Paulo, SP, Brazil) and submitted to a simulation of incipient caries lesions. To simulate caries activity in the oral cavity, a demineralizing solution (DE) and a remineralizing solution (RE) were used. The samples were immersed in 50 ml of the DE solution, composed of CH3COOH 0.075 M. CaCl2 1.0 mM. KH2PO4 2.0 Mm, pH 4.4, for a period of 6 h; they were then removed

and rinsed with distilled water for 10 s. After, they were then placed in 25 mL of the re solution, consisting of KCl 150 mM. CaCl2 1.5 mM. KH2PO4 0.9 mM. NH2C(CH2OH)3 20 Mm, pH 7.0, for a period of 18 h. This protocol was carried out for 7 consecutive days and the solutions were changed daily [21].

Infiltration of resin materials

After simulating the incipient caries lesion, the samples were submitted to the application of the resin infiltrants. The samples were infiltrated according to the manufacturer's instructions for the Icon® resin infiltrant: etching with 15% hydrochloric acid for 2 min, this was followed by washing and drying for 30 seconds each. The following was applied the Icon® Dry (99% ethanol) for 30 s and of the resin infiltrants for 3 min, with removal of excess using a cotton rod and light curing for 40 s (Valo LED, 1000 mW/cm2). Following the manufacturer's recommendations, the resin infiltrant was reapplied for a further 1 min and light-cured for 40 s in each group. The experimental resin infiltrants were applied using a 3 mL disposable syringe, protected from light with a black insulating tape and a free-face applicator tip that comes with the Icon® kit.

Penetration depth

For this analysis. the resin infiltration described above was carried out using the indirect labeling technique [22]. After simulating an incipient caries lesion, the samples from each group (n=5) were conditioned with 15% hydrochloric acid for 2 min; rinsed with a water jet for 30 s and immersed in a 0.1% ethanolic rhodamine B solution (Sigma Aldrich. Steinheim. Germany) for 12 h [23], in order to fill the accessible pores (after demineralization) with rhodamine B for later visualization using confocal microscopy. After 12 hours, the samples were removed from the staining solution, washed and dried for 30 seconds each. Next, Icon® Dry (99% ethanol) was applied for 30 s and the resin infiltrants were applied for 3 min with the excess removed by a cotton rod and light-cured for 40 s (Valo, Ultradent, São Paulo, SP, Brazil). The resin infiltrant was reapplied for another 1 min and light-cured for 40 s. All the infiltrated samples were then cut perpendicular to the surface of the enamel lesion with a diamond disc on a metallographic cutter and polished with 600 and 1200 grit water sandpaper under refrigeration until thin slices with a thickness of 100 µm were achieved. To remove the rhodamine B not adhered to the tooth structure, the slices were immersed in 30% hydrogen peroxide for 12 hours. The samples were then immersed in ethanolic sodium fluorescein solution at 100 µm (NaFl; Sigma Aldrich, Louis, St, USA) for 3 min and washed with distilled water for 30 s. The samples were then taken to the microscope. They were then taken to a Confocal Laser Scanning Microscope (Leica. TCS SP5; Leica. Heidelberg. Germany) with a 63x 1.4NA objective, and immersed in oil in dual fluorescence mode to obtain images.

Color stability

New human tooth samples were fixed to small acrylic plates with sticky wax, leaving only the surface of the polished enamel showing; they were then immersed in a container with 1.5 L of coffee solution, 60 g:1 L (3 Corações®. Sumaré. São Paulo. SP. Brazil) (lot1001078), for a period of 7 days at 37 °C, with daily changes of the coloring solution [17,24]. For the color analyses (n=15), the samples were removed from the acrylic plates, rinsed with distilled water and the color was assessed using a spectrophotometer (Konica Minolta CM-700d, Sensing Americas, Inc, USA) in a light booth (GTI Newburg, NY, USA) in "daily light" mode. A stub was used to accommodate the sample and allow light to pass through from the spectrophotometer. 3 readings of different points on each sample were taken. Color analysis was carried out at three different times: (T1) infiltrated enamel (T2) stained enamel and (T3) polished enamel. The data obtained using the CIEL*a*b* system, which corresponds to L* for luminosity, a* for chromaticity (red-green) and b* (blue-yellow), were also used in the CIEDE2000 color variation formula $\Delta E00 = [(\Delta L'/KLSL)\ 2 + (\Delta C'/KCSC)\ 2 + (\Delta H'/KHSH)\ 2 + RT * (\Delta C'/KCSC) * (\Delta H'/KHSH)]1/2$, between the T1-T2, T2-T3 intervals. The tooth whiteness index (WID) was calculated using the formula WID =0.511 L*-2.324 a*-1.100b*, followed by the index difference (ΔWID) considering the T1-T2, T2-T3 intervals. The perceptibility and acceptability thresholds were followed as described by Paravina et al [25]; thus, for ΔE00, the values are 0.8 for perceptibility and 1.8 for acceptability; and, for the differences in whiteness index (ΔWID) are 0.7 for perceptibility and 2.6 for acceptability [26].

Surface roughness

After the preparation and resin infiltration described above, the human tooth samples were previously fixed (Lysanda, São Paulo, SP, Brazil) on acrylic plates and taken to the roughness meter (Surfcorder, Kosakalab, Toky, Japan), configured with a cut off of 0.25 mm and a reading length of 1.25 mm. The radius of the scanning tip was 2 µm and a speed of 0.1 mm/s [5]. Roughness analyses were also carried out at three different times: (I)

infiltrated enamel (II) stained enamel and (III) polished enamel. For each time, three roughness readings were taken and the averages of each sample (n=15) were obtained.

Statistical Analysis

Data analysis was carried out using R software [27], adopting a 5% significance level for all analyses. Generalized linear models were used to analyze group effects in the sorption, solubility, ΔE00, degree of conversion and contact angle variables. The other variables did not fit a normal distribution and were then analyzed using the non-parametric Kruskal-Wallis and Dunn tests for comparisons between groups and the Friedman and Nemenyi tests for comparisons between times. The variables were described by means, standard deviations, medians, minimum and maximum values.

RESULTS

Degree of conversion (DC) and contact angle (CA)

Table 2 shows the results for the degree of conversion and contact angle of the resin infiltrants evaluated in this study. In terms of degree of conversion, it can be seen that group Base Exp achieved the highest degree of conversion (86.46), followed by 2SnF2 (64.25). The lowest DC was found for 1.5ACP (51.05) and 2ACP (51.33). The group 1SnF2 was statistically equal to Icon. For the contact angle, the lowest value found was associated with Icon (21.17), followed by Base Exp (25.13). The groups with ACP achieved higher CA values when compared to the groups with SnF2.

Table 2. Mean (standard deviation) of degree of conversion and contact angle according to group.

Groups	Degree of conversion (%)	Contact angle (N/m)
	Mean (standard deviation)	Mean (standard deviation)
Icon	54.77 (2.04) d	21.17 (2.52) f
Base Exp	86.46 (2.06) a	25.13 (2.05) e
1ACP	59.33 (2.89) c	34.61 (2.20) b
1.5ACP	51.05 (3.68) e	36.77 (3.31) a
2ACP	51.33 (1.94) e	38.6 (2.36) a
1SnF2	55.60 (2.84) d	27.22 (2.76) d
1.5SnF2	60.49 (4.79) c	27.64 (2.26) d
2SnF2	64.25 (2.08) b	31.29 (2.60) c
p-value	<0.0001	<0.0001

Different vertical letters indicate statistically significant differences ($p \leq 0.05$).

Water sorption (WS) and solubility (SL)

The results of these analyses are shown in Table 3. It can be seen that the lowest water sorption value was observed for Icon (5.78). The group 2ACP obtained a statistically equal result to Base Exp, while 1ACP and 1.5ACP were statistically equal to 2SnF2. The highest sorption value was achieved by 1SnF2 (13.24). For solubility, Icon (0.56) and Base Exp (0.65) obtained the lowest values and were statistically equal to each other. 1ACP and 1.5ACP were statistically equal to 2SnF2. The highest solubility values were found in 1SnF2 (15.29) and 1.5SnF2 (7.11).

Table 3: Mean (standard deviation) of sorption and solubility according to group.

Groups	Sorption (μg/mm³)	Solubility (μg/mm³)
	Mean (standard deviation)	Mean (standard deviation)
Icon	5.78 (0.53) e	0.56 (0.45) e
Base Exp	10.53 (0.63) d	0.65 (0.26) e
1ACP	11.19 (0.67) c	1.98 (0.96) c
1.5ACP	11.51 (1.03) c	2.27 (1.18) c
2ACP	10.69 (0.54) d	1.10 (0.38) d

Groups	Sorption (μg/mm³)	Solubility (μg/mm³)
	Mean (standard deviation)	Mean (standard deviation)
1SnF2	13.30 (0.40) a	15.29 (3.84) a
1.5SnF2	12.15 (0.88) b	7.11 (3.49) b
2SnF2	11.18 (0.64) c	2.23 (1.44) c
p-value	<0.0001	<0.0001

Different vertical letters indicate statistically significant differences ($p \leq 0.05$).

Penetration depth

The qualitative Confocal Laser Scanning Microscopy images of the resin material groups infiltrating the artificial white spot caries lesions can be seen in Figure 1. The representative images show the presence of many filaments, similar to resin tags, in almost all the groups, except for 2SnF2 (Figure 1H), where there is only a thin yellow film superimposed on a green line. Analyzing the microscopic images, it can be seen that the resin tags are not homogeneous in all the groups; this can be seen especially in Figures 1E and 1A, and 1F, referring to 2ACP, Icon, and 1SnF2, respectively. Greenish areas indicate demineralized enamel regions; reddish areas indicate infiltrated regions, and yellowish areas indicate overlapping demineralized and infiltrated regions.

Fig 1 Confocal Laser Scanning Microscopy images of resin infiltration in artificial white spot caries lesions at 63x. (A) Icon. (B) Base Exp. (C) 1ACP. (D) 1.5ACP. (E) 2ACP. (F) 1SnF2. (G) 1.5SnF2. (H) 2SnF2.

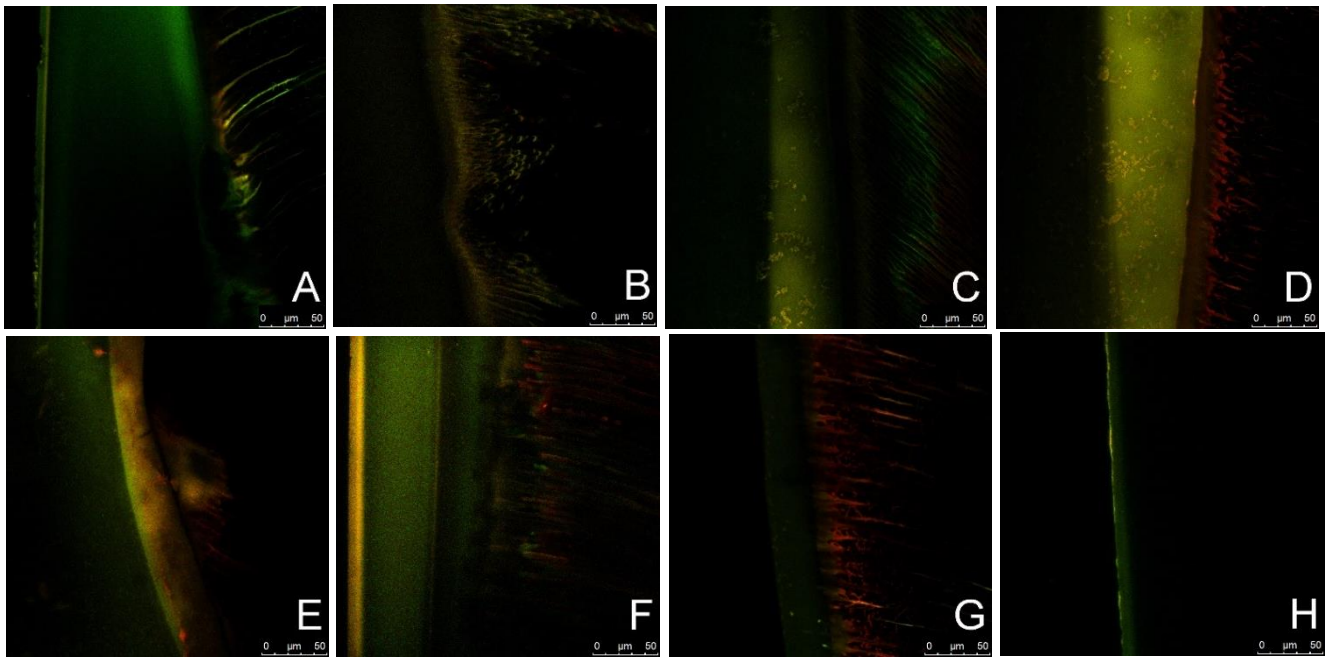

Ion Release

The release of Ca, P and F ions can be seen in Tables 4, 5 and 6. Table 4 shows that all the groups evaluated were statistically equal in the release of Ca ions, for both times evaluated.

Table 4. Median (minimum and maximum value) of Ca release as a function of group and time.

Groups	14 days (ppm)	28 days (ppm)
	Median (minimum and maximum value)	Median (minimum and maximum value)
Icon	0.00 (0.00; 12.00) a	0.00 (0.00; 0.00) a
Base Exp	0.40 (0.00; 14.40) a	0.00 (0.00; 4.90) a
1ACP	0.00 (0.00; 1.10) a	0.00 (0.00; 0.00) a
1.5ACP	0.00 (0.00; 0.00) a	0.00 (0.00; 0.00) a
2ACP	0.00 (0.00; 13.80) a	0.00 (0.00; 1.90) a
1SnF2	0.20 (0.00; 4.90) a	0.00 (0.00; 0.00) a
1.5SnF2	0.00 (0.00; 0.00) a	0.00 (0.00; 0.00) a
2SnF2	0.00 (0.00; 12.50) a	0.00 (0.00; 0.00) a
p-value	0.8303	0.9342

Different vertical letters indicate statistically significant differences ($p \leq 0.05$).

For the P ions (table 5), it was not possible to observe their release. All the groups showed a value of zero and were statistically equal to each other at both times.

Table 5. Median (minimum and maximum value) of P release as a function of group and time.

Groups	14 days (ppm)	28 days (ppm)
	Median (minimum and maximum value)	Median (minimum and maximum value)
Icon	0.00 (0.00; 0.00) a	0.00 (0.00; 0.00) a
Base Exp	0.00 (0.00; 0.00) a	0.00 (0.00; 8.14) a
1ACP	0.00 (0.00; 0.00) a	0.00 (0.00; 11.37) a
1.5ACP	0.00 (0.00; 0.00) a	0.00 (0.00; 0.00) a
2ACP	0.00 (0.00; 43.91) a	0.00 (0.00; 0.00) a
1SnF2	0.00 (0.00; 0.00) a	0.00 (0.00; 0.00) a
1.5SnF2	0.00 (0.00; 0.00) a	0.00 (0.00; 0.00) a
2SnF2	0.00 (0.00; 0.00) a	0.00 (0.00; 0.00) a
p-value	0.9970	0.9842

Different vertical letters indicate statistically significant differences ($p \leq 0.05$).

In relation to fluoride ions (Table 6), the 2SnF2 (17.70) and Icon (0.03) groups were statistically different from each other and from the other groups evaluated over the 14-day period. For the 28-day period, all the groups were statistically the same.

Table 6. Median (minimum and maximum value) of F release as a function of group and time.

Groups	14 days (ppm)	28 days (ppm)
	Median (minimum and maximum value)	Median (minimum and maximum value)
Icon	0.03 (0.02; 0.08) b	0.07 (0.03; 0.08) a
Base Exp	0.07 (0.05; 0.09) ab	0.08 (0.07; 0.10) a
1ACP	0.06 (0.05; 0.07) ab	0.06 (0.03; 0.06) a
1.5ACP	0.06 (0.05; 0.07) ab	0.07 (0.06; 0.07) a
2ACP	0.10 (0.07; 0.13) ab	0.08 (0.07; 0.08) a

Groups	14 days (ppm)	28 days (ppm)
	Median (minimum and maximum value)	Median (minimum and maximum value)
1SnF2	4.10 (1.28; 7.17) ab	0.52 (0.50; 4.50) a
1.5SnF2	1.01 (0.35; 1.36) ab	0.03 (0.03; 6.07) a
2SnF2	17.70 (7.44; 31.92) a	3.42 (2.62; 10.37) a
p-value	0.0080	0.0512

Different vertical letters indicate statistically significant differences ($p \leq 0.05$).

Color stability

The ΔE00 can be found in Table 7. It can be seen that for the T1-T2 interval, the groups with the greatest variation were 1.5SnF2 and 2SnF2, which were statistically similar to each other. The group Icon had the lowest ΔE00 at T1-T2 and was statistically different from all the other groups. 1ACP was statistically the same as Base Exp at T1-T2. For the T2-T3 and T1-T3 intervals, all the groups showed similar behavior, with no statistically significant difference.

Table 7. Mean (standard deviation) of the ΔE00 as a function of the group.

Groups	T1-T2	T2-T3	T1-T3
	Mean (standard deviation)	Mean (standard deviation)	Mean (standard deviation)
Icon	5.56 (2.59) d	8.11 (2.42) a	7.58 (2.95) a
Base Exp	5.91 (3.22) cd	6.93 (1.87) a	6.49 (3.86) a
1ACP	5.86 (3.83) cd	6.17 (2.02) a	6.91 (3.68) a
1.5ACP	7.05 (2.87) bcd	6.3 (1.26) a	7.00 (2.66) a
2ACP	7.79 (2.66) bc	7.1 (1.72) a	9.04 (4.94) a
1SnF2	8.78 (3.79) ab	6.9 (2.55) a	5.23 (2.96) a
1.5SnF2	11.63 (3.35) a	7.19 (2.87) a	6.01 (2.95) a
2SnF2	11.03 (4.29) a	6.67 (2.36) a	7.64 (4.09) a
p-value	<0.001	0.3415	0.1264

Different vertical letters indicate statistically significant differences ($p \leq 0.05$). T1: Infiltrated enamel; T2: Stained enamel; T3: Polished enamel.

The ΔWID can be found in Table 8. It can be seen that in T1, the groups evaluated were statistically the same, with no difference in behavior. In T2, 1ACP was statistically the same as Icon and Base Exp. The groups 1.5SnF2 and 2SnF2 behaved similarly, statistically speaking. It can be seen that groups 1.5SnF2 and 2SnF2 showed more pronounced negative values compared to the other groups evaluated at T2. At T3, the values for all groups were still negative, but less pronounced than at T2 and with no statistically significant difference between the groups.

Table 8. Median (minimum and maximum value) of the ΔWID as a function of the group.

Groups	T1	T2	T3
	Median (minimum and maximum value)	Median (minimum and maximum value)	Median (minimum and maximum value)
Icon	11.67 (-1.67; 18.21) a	0.19 (-21.54; 12.74) a	-0.50 (-12.41; 7.55) a
Base Exp	6.37 (-9.78; 16.89) a	-9.72 (-23.45; 4.39) a	2.13 (-13.32; 9.36) a
1ACP	7.75 (-2.92; 16.39) a	-7.66 (-28.06; 10.92) a	-5.08 (-15.54; 8.65) a
1.5ACP	6.93 (-7.66; 15.79) a	-14.15 (-33.48; 2) ab	-5.80 (-14.40; 10.48) a
2ACP	9.46 (-0.43; 23.82) a	-13.98 (-21.8; 0.8) ab	-6.04 (-16.37; 8.88) a
1SnF2	9.39 (-0.63; 16.43) a	-14.99 (-31.19; -0.85) ab	-0.68 (-14.08; 14.02) a
1.5SnF2	10.52 (-4.54; 20.52) a	-23.19 (-34.53; -6.54) b	-1.01 (-14.37; 12.15) a
2SnF2	8.48 (-6.36; 20.10) a	-23.8 (-34.22; 1.72) b	-4.08 (-13.15; 9.26) a
p-value	0.6007	<0.0001	0.3637

Different vertical letters indicate statistically significant differences ($p \leq 0.05$). T1: Infiltrated enamel; T2: Stained enamel; T3: Polished enamel.

Regarding the ΔL (Table 9) of the groups evaluated, it can be seen that Icon and Base Exp had statistically similar results in the T1-T2 interval. Similarly, 1.5SnF2 and 2SnF2 were also statistically equal to each other and had the highest ΔL when compared to the other groups evaluated. For the T2-T3 interval, 2ACP and Base Exp were statistically the same and statistically different from the other groups. For the T1-T3 interval, all groups were statistically equal.

Table 9. Median (minimum and maximum value) of ΔL as a function of group.

Groups	T1-T2	T2-T3	T1-T3
	Median (minimum and maximum value)	Median (minimum and maximum value)	Median (minimum and maximum value)
Icon	-0.47 (-11.37; 6.52) a	-8.76 (-14.14; 3.28) d	-7.15 (-19.33; -4.65) a
Base Exp	-0.73 (-14.06; 6.15) a	-4.70 (-13.63; 1.12) cd	-6.07 (-19.73; 2.32) a
1ACP	-0.97 (-19.61; 3.11) ab	-4.32 (-11.69; 1.73) bcd	-7.81 (-17.88; 0.75) a
1.5ACP	-2.76 (-13.14; 6.22) ab	-3.59 (-7.88; 2.91) abcd	-7.57 (-16.4; 5.48) a
2ACP	-3.51 (-12.97; 9.65) ab	-5.62 (-11.34; -0.54) cd	-9.14 (-23.29; 2.76) a
1SnF2	-5.68 (-16.25; 3.54) ab	-1.16 (-7.96; 11.73) abc	-3.68 (-13.31; 2.22) a
1.5SnF2	-10.65 (-17.43; 3.26) b	2.79 (-6.38; 13.66) a	-5.69 (-14.57; 2.78) a
2SnF2	-10.92 (-19.58; 2.33) b	-0.05 (-5.42; 10.71) ab	-7.92 (-20.41; -2.5) a
p-value	<0.0001	<0.0001	0.1865

Different vertical letters indicate statistically significant differences ($p \leq 0.05$). T1: Infiltrated enamel; T2: Stained enamel; T3: Polished enamel.

With regard to Δa (Table 10) and Δb (Table 11), the highest values were attributed to the 1.5SnF2 and 2SnF2 groups for the T1-T2 interval. For Δa, 1ACP was statistically equal to Icon and Base Exp in T1-T2; while in T2-T3, 1ACP and 2ACP were statistically equal to Base Exp. For Δb, the 1.5SnF2 group was statistically different from the other groups evaluated in T1-T2 and T2-T3. In T1-T3, the groups were statistically equal in both Δa and Δb. Δb values were higher than Δa values in the T1-T2 interval for all groups tested.

Table 10. Median (minimum and maximum value) of Δa as a function of group.

Groups	T1-T2	T2-T3	T1-T3
	Median (minimum and maximum value)	Median (minimum and maximum value)	Median (minimum and maximum value)
Icon	1.99 (-1.69; 5.10) b	0.36 (-3.54; 2.95) a	2.06 (1.06; 4.16) a
Base Exp	2.23 (-0.49; 7.19) b	-1.13 (-4.00; 0.88) ab	1.13 (-1.08; 3.19) a
1ACP	2.04 (-1.44; 8.01) b	-0.95 (-4.31; 4.31) ab	2.02 (0.14; 6.65) a
1.5ACP	3.96 (-0.09; 7.89) ab	-1.51 (-4.34; 2.32) abc	2.38 (-0.54; 4.18) a
2ACP	3.62 (-0.15; 7.37) ab	-1.05 (-2.9; 1.25) ab	2.32 (-0.32; 7.19) a
1SnF2	3.57 (0.60; 8.01) ab	-3.14 (-6.57; 1.77) bc	1.60 (-0.50; 3.42) a
1.5SnF2	5.28 (2.33; 7.74) a	-3.42 (-6.72; -1.43) c	1.56 (-2.04; 3.19) a
2SnF2	6.10 (0.75; 9.43) a	-3.89 (-7.99; 0.51) c	2.04 (-0.07; 4.91) a
p-value	<0.0001	<0.0001	0.1952

Different vertical letters indicate statistically significant differences (p≤0,05). T1: Infiltrated enamel; T2: Stained enamel; T3: Polished enamel.

Table 11. Median (minimum and maximum value) of Δb as a function of group.

Groups	T1-T2	T2-T3	T1-T3
	Median (minimum and maximum value)	Median (minimum and maximum value)	Median (minimum and maximum value)
Icon	8.98 (-2.16; 17.53) b	-18.59 (-24.42; -10.24) a	1.49 (-4.80; 8.12) a
Base Exp	9.15 (2.10; 14.95) b	-19.76 (-24.44; -14.97) ab	-0.29 (-5.25; 4.93) a
1ACP	7.38 (-0.70; 17.64) b	-18.86 (-28.25; -12.76) ab	3.31 (-2.35; 7.28) a
1.5ACP	11.03 (4.94; 21.14) ab	-22.74 (-27.72; -15.41) abc	2.8 (-5.92; 5.19) a
2ACP	10.62 (2.08; 17.95) ab	-21.64 (-26.54; -11) abc	2.63 (-3.80; 8.81) a
1SnF2	12.23 (3.64; 15.84) ab	-20.74 (-23.89; -14.11) abc	3.92 (-3.17; 7.39) a
1.5SnF2	16.18 (-1.59; 19.03) a	-23.36 (-27.60; -15.96) c	4.14 (-3.10; 10.72) a
2SnF2	13.37 (5.09; 17.79) ab	-23.96 (-28.47; -8.82) bc	0.77 (-4.24; 7.99) a
p-value	<0.0001	0.0001	0.0565

Different vertical letters indicate statistically significant differences (p≤0.05). T1: Infiltrated enamel; T2: Stained enamel; T3: Polished enamel.

Surface Roughness

Table 12 shows the surface roughness values of the groups evaluated. It can be seen that for stained enamel, 1ACP and 2SnF2 were statistically different from all the other groups. Polished enamel showed significantly lower values for all the groups tested, and was statistically different from the other two times evaluated. The 2SnF2 group showed higher roughness values within the three times evaluated, when compared to the other groups. Except for Base Exp and 2SnF2, all the other experimental groups were statistically equal to Icon in polished enamel.

Table 12. Median (minimum and maximum value) roughness as a function of group and time.

Groups	Infiltrated enamel	Stained enamel	Polished enamel	p-value
	Median (minimum and maximum value)	Median (minimum and maximum value)	Median (minimum and maximum value)	
Icon	0.92 (0.50; 1.41) Aab	1.05 (0.59; 1.36) Aab	0.47 (0.19; 0.75) Bab	<0.0001
Base Exp	0.76 (0.35; 1.98) Ab	0.75 (0.45; 1.8) Aab	0.31 (0.19; 0.49) Bb	<0.0001
1ACP	0.77 (0.5; 1.53) Ab	0.74 (0.46; 2.09) Ab	0.41 (0.24; 0.76) Bab	<0.0001
1.5ACP	0.74 (0.54; 1.68) Ab	0.85 (0.39; 1.55) Aab	0.41 (0.16; 0.73) Bab	<0.0001
2ACP	0.94 (0.46; 2.00) Aab	0.94 (0.48; 2.17) Aab	0.36 (0.22; 1.14) Bab	<0.0001
1SnF2	0.99 (0.6; 1.60) Aab	0.93 (0.59; 1.73) Aab	0.43 (0.25; 0.81) Bab	<0.0001
1.5SnF2	0.94 (0.62; 1.70) Aab	0.96 (0.50; 1.73) Aab	0.34 (0.26; 0.8) Bab	<0.0001
2SnF2	1.41 (0.74; 2.70) Aa	1.47 (0.48; 2.37) Aa	0.43 (0.31; 1.10) Ba	<0.0001
p-value	0.0002	0.0387	0.0288	

Different uppercase letters indicate statistically significant differences between the times and lowercase letters indicate statistically significant differences between the groups (p≤0.05).

DISCUSSION

In this study, bioactive particles of amorphous calcium phosphate and tin fluoride were incorporated into experimental resin infiltrant at different concentrations. The hypotheses tested in this study that (I) there would be a difference between the groups in the physical-chemical properties tested and (II) there would be a difference between the times evaluated, were accepted; I saw that there was a statistical difference between the groups for all properties tested and between the times evaluated.

The degree of conversion (DC), which corresponds to the consumption of aliphatic double bonds during monomeric polymerization, has a major influence on the final properties of the resin material [28]. The resin infiltrants studied here contain a large amount of TEGDMA; this monomer has the characteristics of a lower molecular weight and a high degree of conversion. However, in the results presented here, the Icon group, curiously, had the lowest DC value when compared to Exp Base. The manufacturer of the commercial infiltrant reports that the product is composed of 70-95% TEGDMA, however, given the DC results of this study, it is thought that something in its composition may have influenced the result presented here. Previous studies also found lower DC for Icon, with percentages around 56% and even 46% [29,30], corroborating this result. According to the authors, lower DC values for Icon may be related to the large amount of TEGDMA in its composition, which can cause early vitrification, with high monomeric rigidity, during the polymerization reaction and limit adequate conversion of the monomers.

Similarly, the incorporation of bioactive particles considerably reduced the DC for all groups with particles when compared to Exp Base. This may be related to the attenuation of light due to its scattering at the filler/resin interface [31]. Light scattering within the resin material occurs according to the types of monomers and filler used, the filler content and the refractive index of the resin matrix and the filler incorporated [32]. The groups containing ACP particles in this study showed lower DC values when compared to the groups with SnF2. The ACP particles, although nanometric, tend to agglomerate when incorporated into the material, also influencing its viscosity, which could lead to lower molecular mobility and, consequently, lower DC [33]. However, it is known that commercial resin materials with different monomers and fillers in their composition reach a DC of around 50 to 70% [33]. This suggests that the DC values of the infiltrants tested here reached values within what is commercially estimated, which can be considered a favorable result.

The contact angle of a resin material is related to its wettability in relation to a solid surface [34,35]. CA values <90º are desired and considered favorable, meaning that the resin material has good surface wettability; on the other hand, CA >90º would hinder this action, since the material would have little contact with the surface to be infiltrated [36]. It should be considered that the resin infiltrant aims to penetrate the porous body of the incipient caries lesion through capillary forces [2], so it is necessary, among other characteristics, for the material to be able to adequately wet the treated surface in order to achieve successful penetration [37]. It is also known that the incorporation of particles into the material can promote interactions of greater proportion and strength with the resin matrix, providing an increase in CA [38]. In this study, all the groups with added particles had increased CA. The groups with added ACP had higher CA when compared to the groups with SnF2. This may be related to the fact that, even when incorporated in equal quantities by weight, nanoparticles tend to promote greater thickening of the matrix, as previously mentioned, due to their significantly greater total surface area [39]. However, all the CA values obtained were below 90º, as recommended.

In relation to the depth of penetration and homogeneity of the infiltrated materials, it can be seen in figure 1 that most of the groups demonstrated penetrability of the materials in the affected enamel. The TEGDMA monomer has high fluidity and a high penetration coefficient [2,40]. In addition, acid etching plays an important role in the infiltration protocol by permeabilizing the hyper-mineralized layer of the superficial enamel of the white spot lesion [40]. Only the 2SnF2 group showed no resin tags referring to the material penetrated into the enamel subsurface. It is well known that the incorporation of particles increases the viscosity of the infiltrant [7]. Thus, it can be considered that the higher the concentration of incorporated particles, the higher their viscosity tends to be, which could have an impact on the penetrability of the material. In addition, the SnF2 particles may be different in size to the ACP particles. One of the limitations of this study is related to the lack of information from the manufacturer on the size of the SnF2 particles.

Despite the advantages of TEGDMA, this monomer is highly hydrophilic, i.e. it has a high affinity for water and resin materials with a high concentration of TEGDMA may suffer greater water sorption, which would accelerate their degradation when in the oral environment, impacting on their physical properties and, consequently, their longevity [41,42]. Contrary to this statement, the Icon group was the group with the lowest sorption value. Mathias et al. [8] and Souza et al. [7] also found lower water sorption values for Icon, corroborating the results presented here. For some of these authors, the lower sorption value attributed to Icon could be associated

with something in its composition. In relation to the other groups, the addition of particles led to a significant increase in water sorption for almost all the groups when compared to the control groups, except for the 2ACP group, which was statistically the same as the experimental control. Despite the higher sorption results compared to the commercial and experimental controls, all the groups are within the value recommended by ISO 4049/2019, which considers water sorption ≤40μg/mm3 to be ideal [15]. As for solubility, the only group with a solubility value outside that recommended by ISO 4049/2019 (≤7.5μg/mm3) [15] was the 1SnF2 group. These sorption and solubility values may be associated with the residual non-photopolymerized monomers, which hinder the formation of an adequate polymeric network and lead to leaching of its components, promoting greater water sorption and solubility [34].

However, with regard to materials with bioactivity potential, sorption and solubility play an important role in ion exchange with the environment, since this exchange could promote a potential remineralizing effect on dental structures, through the deposition of ions on the surface [42,43]. The release of fluoride ions from dental materials depends on factors related to the individual material and factors related to the oral environment; thus, the characteristics attributed to the material such as composition, charge content and surface exposed to the aqueous environment can affect the release of fluoride ions [44]. Environmental factors include the pH and composition of the immersion medium, as well as the application of the system [44,45,46]. In the results presented here, among the groups with SnF2, only the 2SnF2 group was statistically different from the other groups evaluated, showing fluoride ion release over 14 days in a NaCl solution with an acidic pH. According to the literature, a slower release of fluoride ions has been attributed to the presence of a hydrophobic resin matrix and a relatively low number of fillers [48]. This could explain the results obtained for the groups with SnF2 particles at both times evaluated. Furthermore, no reports were found on the incorporation of SnF2 into the resin infiltrant; therefore, more studies are needed to consolidate the release of fluoride ions and determine the ideal concentration of particles to be incorporated.

As for the release of Ca and P ions, all the groups evaluated were statistically equal. This in vitro study had a small sample size, so given the results found for Ca and P ion release, it cannot be said whether or not there was ion release by the groups evaluated. According to the literature, amorphous calcium phosphate (ACP) is capable of releasing calcium and phosphate ions, favoring the maintenance of a supersaturated state and optimizing the remineralization process of the tooth surface [12,49]. A previous study reported positive results in relation to high levels of ACP release, when 30% of the nanoparticles were incorporated into the commercial resinous infiltrant, including prolonged release [9]. However, higher concentrations of particles could compromise the viscosity and penetration of the material. It is known that low viscosity resin materials should be limited to 15% by weight of filler particles to maintain optimum viscosity and penetration capacity in deep areas of the enamel [50]. It is recommended that further studies be carried out in order to determine the ideal particle concentration to be incorporated into the resin infiltrant and to observe the release of ions and their possible effects on dental enamel.

Evaluating the color stability of a resin infiltrant is important given that incipient caries lesions are not limited to posterior teeth. In addition, its use has been widespread in recent years for the treatment of hypoplastic, hypomineralized and fluorotic lesions; dental conditions that are quite common in anterior teeth and that have great aesthetic involvement [51]. Thus, it is necessary to observe how a new material behaves; analyzing its susceptibility to staining against everyday staining solutions, especially coffee, which is consumed daily throughout the world [6].

It is known that the infiltrant, like any resin material, is susceptible to water sorption and, as a result, the incorporation of dietary pigments and consequent color change can occur [6]. And although most studies use the CIEL*a*b* calculation to determine ΔE for color variation between periods, this study used the CIEDE2000 calculation (ΔE00), considering its greater sensitivity in identifying color changes and mimicking human vision [25]. In the results presented here, it can be seen that almost all the groups with particles had higher ΔE00 in the T1-T2 time interval when compared to the control groups without particles, except for the 1ACP group which was statistically similar to the experimental control. The 1.5SnF2 and 2SnF2 groups achieved the highest ΔE00 in T1-T2 when compared to the other groups. However, the limits of perceptibility (0.8) and acceptability (1.8) for ΔE00 have already been reported and it is assumed that values above this indicate a perceptible color difference that may or may not be clinically acceptable to the observer [25]. The pigmentation of polymeric materials by coffee is explained by the affinity of its pigments with the polymeric phase of the resin material, leading to the absorption of colorants by the material [52]. Previous studies have also used coffee as a coloring agent for infiltrants [10,17]. However, despite the differences between the groups, in the T1-T2 interval of this study, all the groups tested were statistically the same at T2-T3, suggesting that they all behaved similarly when subjected to polishing.

The ΔWID of the samples was also analyzed, an index capable of assessing the reduction in whiteness over time [6]. The results of this study showed that all the groups evaluated reached negative values in T2, indicating a darkening of the samples. The two groups with the highest negative ΔWID values in T2 were the 1.5SnF2 and 2SnF2 groups, corresponding to the groups with the highest SnF2 concentration. Thus, considering the perceptibility (0.7) and acceptability (2.6) values for ΔWID already known in the literature [26], it is thought that the resin infiltrants tested in this study are highly susceptible to staining over time. However, it should be borne in mind that coffee contains a considerable quantity of dyes and [53] is known for its strong and persistent color [54]. For T3, although the negative values reduced considerably, the groups still remained negative when compared to T1; in other words, they were still a little far from white; however, all the groups behaved the same, with no statistically significant difference.

The International Commission on Illumination color system (CIEL*a*b) used in this study is widely used and effective for determining the color changes of resin materials [55,56]. With regard to ΔL, it can be seen that most of the groups evaluated here showed negative ΔL, demonstrating a reduction in luminosity, which correlates with the whiteness index (ΔWID) presented here. The groups with SnF2 particles were the only groups to achieve positive ΔL values in the T2-T3 time interval, suggesting that when they were polished, they were able to re-establish a certain luminosity, related to a clearer surface, but still with low values. With regard to Δa and Δb, there was an increase in values in the groups with particles in the TI-T2 interval. Positive a* values are related to the red pigments contained in the coffee, while positive b* values refer to the yellow pigments in the pigmenting agent [24].

Previous studies have reported that polishing can promote some reversibility of pigmentation [17,57], corroborating this study. The monitoring and polishing of restorative resin materials should be carried out in the dental office by the dentist, so patients should be made aware of the importance of this stage [58]. According to the literature, 1 day of immersion in coffee corresponds to 1 month in vivo [59]. Based on this, the time of exposure to coffee in this study corresponded to a period of 7 months and, in view of the results presented, it is suggested that a control every 6 months should be carried out, since the color stability of the resin infiltrants tested here was relatively low.

Another important property to be analyzed in resin infiltration is surface roughness. Increased roughness can lead to a greater accumulation of plaque in the treated area and, consequently, further demineralization of the surface [60]. Resin infiltration in caries white spot lesions has been shown to reduce enamel surface roughness [61,62] and is considered clinically acceptable [63]. However, it is also important to evaluate the behavior of these materials in relation to staining solutions, since, in the case of an aqueous medium and a material susceptible to water sorption, changes can occur not only in color, but also in roughness. The results shown in Table 12 show that immersion in coffee for 7 days was able to significantly alter the roughness of groups 1ACP and 2SnF2 when compared to the other groups; all the other experimental groups were statistically equal to the commercial and experimental controls when subjected to staining. For the times evaluated, polished enamel was statistically different from the other two, considerably reducing the roughness values of the groups evaluated. Furthermore, it is already known that the perception of roughness in vivo normally occurs when the Ra value is greater than 0.5 μm [5]. In this study, all the groups evaluated had values ≤0.5 μm after surface polishing.

The resin infiltrant has gained ground in Minimally Invasive Dentistry, its main advantage being the preservation of sound enamel adjacent to incipient caries lesions [4]. However, the search for improvements and refinement of this material has been encouraged [5,6,7,8,16], with the belief that the material has the potential to deliver better performance in the treatment of white spot lesions. From the results presented here, it can be inferred that the addition of particles to the resin infiltrant was able to alter the physical properties of the resin material in question, however, many changes remain within the recommended values, or are subject to improvement, when submitted to professional monitoring and polishing.

CONCLUSION

The addition of bioactive particles generally reduced the degree of conversion and increased the contact angle, water absorption and solubility. The group with 2% SnF2 was the only group that did not show infiltration in the artificial white spot lesion. The 2SnF2 group was able to release fluoride ions. Despite the low color stability of the experimental groups with particles, polishing promoted a certain color reversibility, removing pigments from the surface and reducing surface roughness.

REFERENCES

1. Ferreira JD, Flor-Ribeiro MD, Marchi GM, Pazinatto FB (2019) The use of resinous infiltrants for the management of incipient carious lesions: A literature review. J Health Sci 21(4): 358-64.
2. Lasfargues JJ, Bonte E, Guerrieri A, Fezzani L (2013) Minimal intervention dentistry: Part 6. Caries inhibition by resin infiltration. Br Dent J 214(2):53-9.
3. Peters MC, Hopkins AR, Zhu L, Yu Q (2019) Efficacy of Proximal Resin Infiltration on Caries Inhibition: Results from a 3-Year Randomized Controlled Clinical Trial. J Dent Res 98:1497–502.
4. Paris S, Bitter K, Krois J, Meyer-Lueckel H (2020) Seven-year-efficacy of proximal caries infiltration – Randomized clinical trial. J Dent 93:7–10.
5. de Cerqueira GA, Damasceno JE, Pedreira PR, Souza AF, Aguiar FHB, Marchi MG (2023) Roughness and Microhardness of Demineralized Enamel Treated with Resinous Infiltrants and Subjected to an Acid Challenge: An in vitro Study. Open Dent J https://doi.org/10.2174/18742106-v17-230223-2022-126.
6. Zago JLG, de Cerqueira GA, Ferreira RS, Aguiar FHB, Tabchoury CPM, Marchi GM (2023) Evaluation of experimental infiltrant containing nanohydroxyapatite on color stability and microhardness in demineralized enamel. Clin Oral Investig https://doi.org/10.1007/s00784-023-05298-3.
7. Souza AF, Souza MT, Damasceno JE, Ferreira PVC, de Cerqueira GA, Aguiar FHB. Marchi GM (2023) Effects of the Incorporation of Bioactive Particles on Physical Properties, Bioactivity and Penetration of Resin Enamel Infiltrant. Clin Cosmet Investig Dent 15:31-43.
8. Mathias C, Gomes RS, Dressano D, Braga RR, Aguiar FHB, Marchi GM (2019) Effect of diphenyliodonium hexafluorophosphate salt on experimental resin infiltrants containing different diluents. Odontology 107:202-8.
9. Zixiang Dai a, Xianju Xie a, Ning Zhang a, Song Li a, Kai Yang a, Minjia Zhu a (2022) Novel nanostructured resin infiltrant containing calcium phosphate nanoparticles to prevent enamel white spot lesions. J Mech Behav Biomed Mater 126(104990):1-9.
10. Ayad AH, AbdelHafez MI, AlGhandour RN, Mustafa DS, Nour KA (2022) Effect of different surface treatments on the microhardness and colour change of artificial enamel lesions. Aust dent J 0:1-9.
11. Lale S, Solak H, Hınçal E, Vahdettin L (2020) In Vitro Comparison of Fluoride, Magnesium, and Calcium Phosphate Materials on Prevention of White Spot Lesions around Orthodontic Brackets. Biomed Rest J 1-11.
12. Fernando JR, Shen P, Sim CPC, Chen Y, Walker GD, Yuan Y (2019) Self-assembly of dental surface nanoflaments and remineralisation by SnF2 and CPP-ACP nanocomplexes. Sci Rep 9(1):1285.
13. Skucha-Nowak M, Machorowska-Pieniążek A, Tanasiewicz M (2016) Assessing the penetrating abilities of experimental preparation with dental infiltrant features using optical microscope: preliminary study. Adv Clin Exp Med 25(5):961-969.
14. Souza EJ, Prieto LT, Soares GP, Dos Santos Dias CT, Aguiar FHB, Paulillo LAMS (2012) The effect of curing light and chemical catalyst on the degree of conversion of two dual cured resin luting cements. Lasers Med Sci 27:145–51. https://doi.org/10.1007/s10103-010-0857-y.
15. De Cerqueira GA, Souza LS, Gomes RS, Marchi GM, Mathias P (2020) Effect of ceramic thicknesses and opacities on water sorption and solubility of a light-curing resin cement by different units. Bras J Oral Sci 20:1-13.
16. Pedreira PR, Damasceno JE, Mathias C, Sinhoreti MAC, Aguiar FHB, Marchi GM (2021) Influence of Incorporating Zirconium- and Barium-based Radiopaque Filler Into Experimental and Commercial Resin infiltrants. Oper Dent 46(5):566-576.
17. Leland A, Akyalcin S, English JD, Tufekci E, Paravina R (2016) Evaluation of staining and color changes of a resin infiltration system. Angle Orthod 86(6):900–904.
18. Alqahtani S, Abusaq A, Alghamdi M, Shokair N, Albounni R (2022) Color stability of resin infiltrated white spot lesion after exposure to stain-causing drinks. Saudi J Biol Sci 29(2):1079-1084. https://doi.org/10.1016/j.sjbs.2021.09.063.
19. Sang EJ, Song JS, Chung SH, Jin BH, Hyun HK (2021) Influence of a new polishing system on changes in gloss and surface roughness of resin composites after polishing and brushing. Dent Mater J 40(3):727-35.

20. Ashwath B, Vijayalakshmi R, Arun D, Kumar V (2014) Site-based plaque removal efficacy of four branded toothbrushes and the effect of dental floss in interproximal plaque removal: A randomized examiner-blind controlled study. Quintessence Int 45(7):577-84.
21. Al-Obaidi R, Salehi H, Desoutter A, Tassery H, Cuisinier F (2019) Formation and assessment of enamel subsurface lesions in vitro. J Oral Sci 61:454-8.
22. Paris S, Bitter K, Renz H, Hopfenmuller W, Meyer-Lueckel H (2009) Validation of two dual fluorescence techniques for confocal microscopic visualization of resin penetration into enamel caries lesions. Microsc Res Tech 72(7):489-94.
23. D'Alpino PH, Pereira JC, Rueggeberg FA, Svizero NR, Miyake K, Pashley DH (2006) Efficacy of composite surface sealers in sealing cavosurface marginal gaps. J Dent 34(3):252-9.
24. Ceci M, Rattalino D, Viola M, Beltrami R, Chiesa M, Colombo M, Poggio C (2017) Resin infiltrant for non-cavitated caries lesions: evaluation of color stability. J Clin Exp Dent 9(2):e231– e237.
25. Paravina RD, Pérez MM, Ghinea R (2019) Acceptability and perceptibility thresholds in dentistry: a comprehensive review of clinical and research applications. J Esthet Restor Dent 31(2):103– 112.
26. Pérez MM, Herrera LJ, Carrillo F, Pecho OE, Dudeia D et al (2019) Whiteness diference thresholds in dentistry. Dent Mater 35(2):292–297.
27. R Core Team (2024). R: A language and environment for statistical computing. R Foundation for Statistical Computing, Vienna, Austria.
28. Fonseca ASQS, Labruna Moreira AD, De Albuquerque PPAC, de Menezes LR, Pfeifer CS, Schneider LFJ (2017) Effect of monomer type on the CC degree of conversion, water sorption and solubility, and color stability of model dental composites. Dent Mater 33(4):394–401. https://doi.org/10.1016/j.dental.2017.01.010.
29. Obeid AT, Garcia LHA, Nascimento TRL, Castellano LRC, Bombonatti JFS, Honório HM et al (2022) Effects of hybrid inorganic-organic nanofibers on the properties of enamel resin infiltrants - An in vitro study. J Mech Behav Biomed Mater 126:105067. https://doi.org/10.1016/j.jmbbm.2021.105067.
30. Prodan D, Moldovan M, Chisnoiu AM, Saroși C, Cuc S, Filip M, Gheorghe GF et al (2022) Development of New Experimental Dental Enamel Resin Infiltrants-Synthesis and Characterization. Materials (Basel) 15(3):803. https://doi.org/10.3390/ma15030803.
31. Par M, Spanovic N, Bjelovucic R, Skenderovic H, Gamulin O, Tarle Z (2018) Curing potential of experimental resin composites with systematically varying amount of bioactive glass: Degree of conversion, light transmittance and depth of cure. J Dent 75:113-20.
32. Moldovan M, Balazsi R, Soanca A, Roman A, Sarosi C, Prodan D et al (2019) Evaluation of the Degree of Conversion, Residual Monomers and Mechanical Properties of Some Light-Cured Dental Resin Composites. Materials 12:2109.
33. Par M, Gamulinb O, Marovicc D, Skenderovicd H, Klaricc E, Tarlec Z (2016) Conversion and temperature rise of remineralizing composites reinforced with inert fillers. J Dent 48:26-33.
34. Van Landuyt KL, Snauwaert J, De Munck J, Peumans M, Yoshida Y, Poitevin A, Coutinho E et al (2007) Systematic review of the chemical composition of contemporary dental adhesives. Biomaterials 28(26):3757-85. doi: 10.1016/j.biomaterials.2007.04.044.
35. Cibim DD, Inagaki LT, Dainezi VB, Pascon FM, Alonso RC, Kantoviz KR, Puppin-Rontani RM (2017) Wettability Analysis of Experimental Resin Infiltrants Containing Chlorhexidine. Austin Dent Sci 2(1):1011.
36. Yuan Y, Lee TR (2013) Contact Angle and Wetting Properties. In: Bracco G., Holst B. (eds) Surface Science Techniques. Springer, Berlin, Heidelberg 51. https://doi.org/doi.org/10.1007/978-3-642-34243-1_1
37. Gaglianone LA, Pfeifer CS, Mathias C, Puppin-Rontani RM, Marchi GM (2020) Can composition and preheating improve resin infiltrant characteristics and penetrability in demineralized enamel? Braz Oral Res 34:1–11.
38. Kim JS, Cho BH, Lee IB, Um CM, Lim BS, Oh MH, Chang CG, Son HH (2005) Effect of the hydrophilic nanofiller loading on the mechanical properties and the microtensile bond strength of an ethanol-based one-bottle dentin adhesive. J Biomed Mater Res B Appl Biomater 72(2):284-91. https://doi.org/10.1002/jbm.b.30153.

39. Bastos NA, Bitencourt SB, Martins EA, De Souza GM (2020) Review of nano-technology applications in resin-based restorative materials. J Esthet Restor Dent 2020:1–16.
40. Meyer-Lueckel, Hendrik Paris S (2008) Resin Infiltration of Natural Caries Lesions :1112–7.
41. Mandava J, Reddy YS, Kantheti S, Chalasani U, Ravi RC, Borugadda R et al (2017) Microhardness and Penetration of Artificial White Spot Lesions Treated with Resin or Colloidal Silica Infiltration. J Clin Diagn Res 11(4):ZC142-ZC146.
42. Sfalcin RA, Correr1 AB, Morbidelli LR, Araújo TGF, Feitosa VP, Correr-Sobrinho L et al (2017) Influence of bioactive particles on the chemical-mechanical properties of experimental enamel resin infiltrants. Clin Oral Investig 21:2143-51.
43. Sauro S, Osorio R, Fulgencio R,Watson TF, Cama G, Thompson I, Toledano M (2013) Remineralisation properties of innovative light-curable resin-based dental materials containing bioactive micro-fillers. J Mater Chem B 1: 2624–38.
44. Kelić K, Par M, Peroš K, Šutej I, Tarle Z (2020) Fluoride-Releasing Restorative Materials: The Effect of a Resinous Coat on Ion Release. Acta Stomatol Croat 54(4):371-381.
45. Wiegand A, Buchalla W, Attin T (2007) Review on fluoride-releasing restorative materials--fluoride release and uptake characteristics, antibacterial activity and influence on caries formation. Dent Mater 23(3):343-62.
46. Mazzaoui SA, Burrow MF, Tyas MJ (2000) Fluoride release from glass ionomer cements and resin composites coated with a dentin adhesive. Dent Mater 16(3):166-71.
47. Bell A, Creanor SL, Foye RH, Saunders WP (1999) The effect of saliva on fluoride release by a glass-ionomer filling material. J Oral Rehabil 26(5):407-12.
48. Yap AU, Tham SY, Zhu LY, Lee HK (2002) Short-term fluoride release from various aesthetic restorative materials. Oper Dent 27(3):259-65.
49. Cochrane NJ, Saranathan S, Cai F, Cross KJ, Reynolds EC (2008) Enamel subsurface lesion remineralisation with casein phosphopeptide stabilised solutions of calcium, phosphate and fluoride. Caries Res 42:88-97.
50. Van Landuyt KL, Snauwaert J, De Munck J, Peumans M, Yoshida Y, Poitevin A, et al (2007) Systematic review of the chemical composition of contemporary dental adhesives. Biomater 28:3757-85.
51. Damasceno JE, Pedreira PR, de Cerqueira GA, Souza AF, Zago JLG, Aguiar FHB, Marchi GM (2022) Resin infiltrant as a treatment of common changes in dental enamel: narrative literature review. Res Soc Dev 11(7):e54411730143.
52. Kentrou C, Papadopoulos T, Lagouvardos P (2014) Color changes in staining solutions of four light-cured indirect resin composites. Odontology 102(2):189-96. https://doi.org/10.1007/s10266-013- 0106-5.
53. Moon JD, Seon EM, Son SA, Jung KH, Kwon YH, Park JK (2015) Effect of immersion into solutions at various pH on the color stability of composite resins with different shades. Restor Dent Endod 40(4):270-6. https://doi.org/10.5395/rde.2015.40.4.270.
54. Alkhadim YK, Hulbah MJ, Nassar HM (2020) Color shift, color stability, and post-polishing surface roughness of esthetic resin composites. Materials (Basel) 13(6). https://doi.org/10.3390/ ma13061376.
55. Inokoshi S, Burrow MF, Kataumi M, Yamada T, Takatsu T (1996) Opacity and color changes of tooth-colored restorative materials. Oper Dent 21(2):73-80.
56. Celik C, Yuzugullu B, Erkut S, Yamanel K (2008) Effects of mouth rinses on color stability of resin composites. Eur J Dent 2(4):247-53.
57. Kobbe C, Fritz U, Wierichs RJ, Meyer-Lueckel H (2019) Evaluation of the value of re-wetting prior to resin infiltration of post orthodontic caries lesions. J Dent 91:103243. https://doi.org/10. 1016/j.jdent.2019.103243.
58. Mazur M, Westland S, Ndokaj A, Nardi GM, Guerra F, Ottolenghi L (2022) In-vivo colour stability of enamel after ICON® treatment at 6 years of follow-up: a prospective single center study. J Dent 122:103943. https://doi.org/10.1016/j.jdent.2021.103943.
59. Ertaş E, Güler AU, Yücel AC, Köprülü H, Güler E (2006) Color stability of resin composites after immersion in diferent drinks. Dent Mater J 25(2):371–376.
60. Arnold WH, Meyer A-K, Naumova EA (2016) Surface Roughness of Initial Enamel Caries Lesions in Human Teeth After Resin Infiltration. Open Dent J 10:505–15. https://doi.org/10.2174/1874210601610010505.

61. El Meligy OAES, Alamoudi NM, Eldin Ibrahim ST, Felemban OM, Al-Tuwirqi AA (2021) Effect of resin infiltration application on early proximal caries lesions in vitro. J Dent Sci 16:296–303. https://doi.org/10.1016/j.jds.2020.04.005.
62. Soveral M, Machado V, Botelho J, Mendes JJ, Manso C (2021) Effect of resin infiltration on enamel: A systematic review and meta-analysis. J Funct Biomater 12. https://doi.org/10.3390/jfb12030048.
63. Taher NM, Alkhamis HA, Dowaidi SM (2012) The influence of resin infiltration system on enamel microhardness and surface roughness: An in vitro study. Saudi Dent J 24:79–84. https://doi.org/10.1016/j.sdentj.2011.10.003.

3 CONCLUSÃO

A adição de ACP no infiltrante resinoso não foi relevante, diferentemente do fluoreto de estanho que se mostrou promissor devido à sua liberação iônica. A adição das partículas reduziu o grau de conversão e aumentou a sorção de água e solubilidade. Alterações de cor foram potencializadas nos mateiais com partículas incorporadas, contudo minimizadas pelo polimento.

[1]REFERÊNCIAS*

Abbas BA, Marzouk ES, Zaher AR. Treatment of various degrees of white spot lesionsusing resin infiltration-in vitro study. Prog Orthod. 2018;19(1):27.

Askar H, Schwendicke F, Lausch J, Meyer-Lueckel H, Paris S. Modified resin infiltrationof non-, micro- and cavitated proximal caries lesions in vitro. J Dent. 2018;74:56-60.

Babcock FD, King JC, Jordan TH. The reaction of stannous fluoride and hydroxyapatite. J Dent Res. 1978;57(9):933-8.

Cheng X, Liu J, Li J, Zhou X, Wang L, Liu J et al. Comparative effect of a stannous fluoride toothpaste and a sodium fluoride toothpaste on a multispecies biofilm. Arch Oral Biol. 2017;74:5-11.

Cochrane NJ, Saranathan S, Cai F, Cross KJ, Reynolds EC. Enamel subsurface lesion remineralisation with casein phosphopeptide stabilised solutions of calcium, phosphate and fuoride. Caries Res. 2008;42:88-97.

Cross KJ, Huq NL, Reynolds EC. Casein phosphopeptides in oral health–chemistry and clinical applications. Curr. Pharm. Des. 2007;13:793-800.

De Rooij JF, Nancollas GH. The formation and remineralization of artificialwhite spot lesions: A constant composition approach. J Dent Res. 1984;63:864-867.

Ekstrand KR, Bakhshandeh A, Martignon S. Treatment of proximal superficial caries lesions on primary molar teeth with resin infiltration and fluoride varnish versus fluoridevarnish only: efficacy after 1 year. Caries Res. 2010;44(1):41-6.

Faller RV, Eversole SL. Protective effects of SnF2 - Part III. Mechanism of barrier layer

* De acordo com as normas da UNICAMP/FOP, baseadas na padronização do International Committee of Medical Journal Editors - Vancouver Group. Abreviatura dos periódicos em conformidade com o PubMed.

attachment. Int Dent J. 2014;64:16-21.

Fan M, Yang J, Xu HHK, Weir MD, Tao S, Yu Z et al. Remineralization effectiveness of adhesive containing amorphous calcium phosphate nanoparticles on artificial initial enamel caries in a biofilm-challenged environment. Clin Oral Investig. 2021;25(9):5375-5390.

Fernando JR, Shen P, Sim CPC, Chen Y, Walker GD, Yuan Y. Self-assembly of dental surface nanofilaments and remineralisation by SnF2 and CPP-ACP nanocomplexes. Sci Rep. 2019;9(1):1285.

Gaglianone LA, Pfeifer CS, Mathias C, Puppin-Rontani RM, Marchi GM. Can composition and preheating improve resin infiltrant characteristics and penetrability in demineralized enamel? Braz Oral Res. 2020;34:1–11.

Ganss C, Hardt M, Lussi A, Cocks AK, Klimek J, Schlueter N et al. Mechanism of action of tin-containing fluoride solutions as anti-erosive agents in dentine - an in vitro tin-uptake, tissue loss, and scanning electron microscopy study. Eur J Oral Sci. 2010;118:376-384.

Gao Y, Liang K, Weir MD, Gao J, Imazato S, Tay FR et al. Enamel remineralization via poly(amido amine) and adhesive resin containing calcium phosphate nanoparticles. J Dent. 2020;92:103262.

Golz L, Simonis RA, Reichelt J, Stark H, Frentzen M, Allam JP, et al. In vitro biocompatibility of ICON and TEGDMA on human dental pulp stem cells. Dent Mater. 2016;32:1052–64.

Konradsson K, Lingstron P, Emilson C, Johannsen G, Ramberg P, Johannsen A. Stabilized stannous fluoride dentifrice in relation to dental caries, dental erosion and dentin hypersensitivity: A systematic review. Am J Dent. 2020;33(2):96-105.

Lasfargues JJ, Bonte E, Guerrieri A, Fezzani L. Minimal intervention dentistry: Part 6. Caries inhibition by resin infiltration. Br Dent J. 2013;214:53-9.

Mandava J, Reddy YS, Kantheti S, Chalasani U, Ravi RC, Borugadda R et al.Microhardness and Penetration of Artificial White Spot Lesions Treated with Resin or Colloidal Silica Infiltration. J Clin Diagn Res. 2017;11(4):ZC142-ZC146.

Mathias C, Gomes RS, Dressano D, Braga RR, Aguiar FHB, Marchi GM. Effect of diphenyliodonium hexafluorophosphate salt on experimental resin infiltrants containing different diluents. Odontology. 2019;107:202-8.

Par M, Spanovic N, Bjelovucic R, Skenderovic H, Gamulin O, Tarle Z. Curing potential of experimental resin composites with systematically varying amount of bioactive glass: Degree of conversion, light transmittance and depth of cure. J Dent. 2018;75:113-20.

Paris S, Hopfenmuller W, Meyer-Lueckel H. Resin infiltration of caries lesions: an efficacy randomized trial. J Dent Res. 2010;89(8):823-6.

Paris S, Bitter K, Krois J, Meyer-Lueckel H. Seven-year-efficacy of proximal caries infiltration – Randomized clinical trial. J Dent 2020;93:7–10.

Pedreira PR, Damasceno JE, Mathias C, Sinhoreti MAC, Aguiar FHB, Marchi GM. Influence of Incorporating Zirconium- and Barium-based Radiopaque Filler Into Experimental and Commercial Resin infiltrants. Oper Dent. 2021;46(5):566-576.

Peters MC, Hopkins AR, Zhu L, Yu Q. Efficacy of Proximal Resin Infiltration on Caries Inhibition: Results from a 3-Year Randomized Controlled Clinical Trial. J Dent Res. 2019;98:1497–502.

Pitts NB, Zero DT, Marsh PD, Ekstrand K, Weintraub JA, Ramos-Gomez F et al. Dental Caries. Nat Rev Dis Primers. 2017;3(17030):1-16.

Phark JH, Duarte S, Meyer-Lueckel H, Paris S. Caries infiltration with resins: a novel treatment option for interproximal caries. Compend Conti Educ Dent. 2009;30:13-17.

Prajapati D, Nayak R, Pai D, Upadhya N, K Bhaskar V, Kamath P. Effect of Resin Infiltration on Artificial Caries: An in vitro Evaluation of Resin Penetration and Microhardness. Int J Clin Pediatr Dent. 2017;10(3):250-256.

Sfalcin RA, Correr1 AB, Morbidelli LR, Araújo TGF, Feitosa VP, Correr-Sobrinho L et al. Influence of bioactive particles on the chemical-mechanical properties of experimental enamel resin infiltrants. Clin Oral Investig. 2017;21:2143-51.

Sideridou I, Tserki V, Papanastasiou G. Effect of chemical structure on degree of conversion in light-cured dimethacrylate-based dental resins. Biomaterials. 2002;23:1819-29.

Schlueter N, Duran A, Klimek J, Ganss C. Investigation of the effect of various fluoride compounds and preparations thereof on erosive tissue loss in enamel in vitro. Caries Res. 2009;43:10-16.

Schlueter N, Engelmann F, Klimek J, Ganss C, Hardt M, Lussi A. Tin-cotaining fluoride solutions as anti-erosive agents in enamel: An in vitro tin-uptake, tissue-loss, and scanning electron micrograph study. Eur J Oral Sci. 2009;117(4):427-34.

Skucha-Nowak M, Machorowska-Pieniążek A, Tanasiewicz M. Assessing the penetrating abilities of experimental preparation with dental resin infiltrant features using optical microscope: preliminary study. Adv Clin Exp Med. 2016;25(5):961-969.

Urquhart O, Tampi MP, Pilcher L, Slayton RL, Araujo MWB, Fontana M. Nonrestorative Treatments for Caries: Systematic Review and Network Meta-analysis. J Dent Res. 2019;98(1):14-26.

Yanwei Yang a, Zexian Xu, Yuqing Guo, Hongchen Zhang, Yinong Qiu, Jianxue Li. Novel core–shell CHX/ACP nanoparticles effectively improve the mechanical, antibacterial and

remineralized properties of the dental resin composite. Dent Mater. 2021;37:636–647.

Zixiang Dai a, Xianju Xie a, Ning Zhang a, Song Li a, Kai Yang a, Minjia Zhu a. Novel nanostructured resin infiltrant containing calcium phosphate nanoparticles to prevent enamel white spot lesions. J Mech Behav Biomed Mater. 2022;126(104990):1-9.

APÊNDICE 1: Metodologia Ilustrada

Formulação dos infiltrantes

As composições dos infiltrantes resinosos são mostradas na Tabela 1, todas em porcentagem em peso. Uma balança de precisão (Shimadzu, Tóquio, Japão) foi utilizada para pesar os reagentes sob luz amarela. A seguir, cada recipiente com a mistura de reagentes foi levado ao speedmixer (Hauschild, Farmington Hills, EUA) sob 3000 RPMs, por 5 minutos, para homogeneização dos componentes. Ao final, os infiltrantes resinosos foram armazenados individualmente sob refrigeração a 4 ºC. As concentrações de partículas foram obtidas em estudo piloto prévio, com base na viscosidade dos infiltrantes após incorporação das partículas.

Tabela 1 – Descrição dos grupos e composição dos resin infiltrantes resinosos avaliados.

Grupos	Composição dos infiltrantes
Icon (controle comercial)	Icon® (70-95% TEGDMA, <2.5% CQ e aditivos)
Exp Base (controle experimental)	98,5% TEGDMA-BisEMA; 0.5% CQ; 1% EDAB
1ACP	97,5% TEGDMA-BisEMA; 0.5% CQ; 1% EDAB; 1% ACP
1.5ACP	97% TEGDMA-BisEMA; 0.5% CQ; 1% EDAB; 1.5% ACP
2ACP	96,5% TEGDMA-BisEMA; 0.5% CQ; 1% EDAB; 2% ACP
1SnF2	97,5% TEGDMA-BisEMA; 0.5% CQ; 1% EDAB; 1% SnF2
1.5SnF2	97% TEGDMA-BisEMA; 0.5% CQ; 1% EDAB; 1.5% SnF2
2SnF2	96,5% TEGDMA-BisEMA; 0.5% CQ; 1% EDAB; 2% SnF2

Icon®, de acordo com o fabricante (DMG, Hamburgo, Alemanha) (LOT 261398). BisEMA - Dimetacrilato de polietilenoglicol Bisfenol A (Sigma Aldrich Brasil Ltda, Barueri, SP, Brasil). TEGDMA - Dimetacrilato de trietilenoglicol (Sigma Aldrich Brasil Ltda, Barueri, SP, Brasil). CQ – Canforquinona (Sigma Aldrich Brasil Ltda, Barueri, SP, Brasil). EDAB - Benzoato de etil 4-dimetilamino (Sigma Aldrich Brasil Ltda, Barueri, SP, Brasil). ACP - Fosfato de cálcio amorfo (Sigma Aldrich Brasil Ltda, Barueri, SP, Brasil) (<150nm) e SnF2 - Fluoreto de estanho PA (Êxodo Científica, Sumaré, SP, Brasil).

Grau de conversão (CD)

Espectroscopia infravermelha por transformada de Fourier com refletância total atenuada (FTIR-ATR) (espectrômetro Vertex 70, Bruker, Billerica, MA, EUA) (Figura 1) foi

utilizada para o CD (n=5). A primeira leitura do material resinoso, ainda não fotopolimerizado, foi feita depositando-se cerca de 1μL dos infiltrantes resinosos no cristal do aparelho, por meio de uma pipeta, de modo que a gota permanecesse no centro focal do feixe de laser do equipamento. Uma tira de poliéster foi então colocada sobre a microgota de material para padronizar as amostras. O material foi fotopolimerizado utilizando fonte de luz LED (Valo, Ultradent, Indaiatuba, SP, Brasil) com densidade de potência de 1000mW/cm2, por 40 segundos. Uma segunda leitura foi realizada após 2 minutos de espera. O software Opus v.6 (Bruker Optics) foi utilizado para calcular o grau de conversão (em%). A linha de base correspondente foi traçada e o valor de absorbância da linha de base foi subtraído do valor máximo de absorbância no número de onda correspondente; Os comprimentos de onda utilizados para obter os valores foram 1610 e 1637.

Figura 1 – (A) Espectrofotômetro de infravermelho por transformador de Fourier. (B) Cristal do aparelho. (C) Aparato com fita adesiva criado para leitura preliminar com feixe incidindo no centro da amostra.

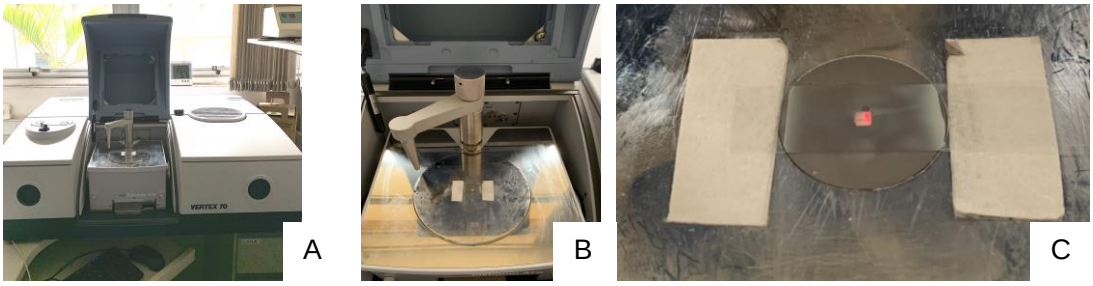

Fonte: Autores

Ângulo de contato (AC)

As mensurações do ângulo de contato foram realizadas em lâmina de vidro polida, limpa com álcool absoluto e seca em estufa a 37ºC por 24 horas, trocando a lãmina a cada análise. Um goniômetro com câmera acoplada (Ramé-hart - 500F1, Succasunna, EUA) (Figura 2) foi utilizado para medir o ângulo de contato dos infiltrantes resinosos. Para isso, gotas de aproximadamente 1μL foram dispensadas perpendicularmente na superfície da lâmina de vidro, por meio de uma micro seringa de precisão. As imagens foram obtidas a partir de 10 mensurações por amostra, com intervalo de tempo de 0,05 segundos e média de 60 frames/segundo. As imagens obtidas foram analisadas utilizando o software de análise de formato de gota (DROPimage Advanced). Para cada grupo (n=16), foi calculada a média dos ângulos de contato de cada lado da gota em graus.

Figura 2 – (A) Goniômetro com câmera acoplada. (B) Seringa com isolamento de luz, contendo os infiltrantes,

acoplada ao dispositivo do equipamento; (C) Imagem da gota do infiltrante.

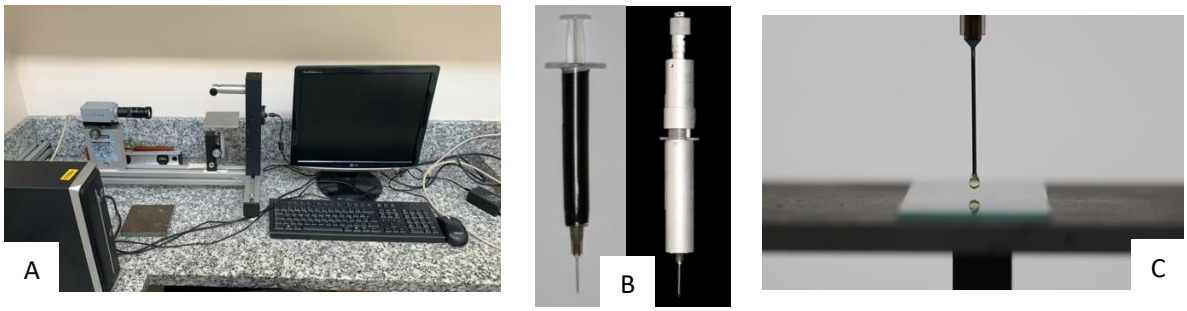

Fonte: Autores

Sorção de água (So) e Solubilidade (SL)

Amostras em forma de disco (5mm x 1mm) dos infiltrantes resinosos (n=16) foram confeccionadas com matriz de silicone e polimerizadas com luz Valo LED (Valo, Ultradent, Indaiatuba, SP, Brasil), com densidade de potência de 1000mW/cm2, por 40 segundos; em seguida, foram colocadas em dessecador e armazenadas em estufa a 37º C. As amostras foram pesadas diariamente em balança analítica (Shimadzu, Tóquio, Japão), em intervalos de 24 horas, até a obtenção de massa constante (m1), com variação inferior a 0,002 mg. Para o cálculo do volume (mm^3), cada amostra teve sua espessura e diâmetro medidos com paquímetro digital (Mitutoyo, Japão). As amostras foram, então, armazenadas a 37ºC em eppendorfs fechados contendo 1,5 mL de água destilada. Após sete dias de armazenamento, os eppendorfs foram retirados da estufa e deixados em temperatura ambiente por 30 minutos; as amostras foram, então, secadas suavemente com papel absorvente e, novamente pesadas em balança analítica para obtenção de m2. Após esse período, as amostras foram dessecadas e pesadas novamente, diariamente, até a obtenção de nova massa constante (m3). Os valores de sorção e solubilidade foram calculados utilizando duas fórmulas específicas (So= m2-m3/V e SL= m1-m3/V), de acordo com a especificação ISO 4049/2019.

Figura 3 – (A) Matriz de teflon em formato cilíndrico; Molde de silicone com formato cilíndrico e amostras finalizadas após polimerização. (B) Balança Analítica de Alta Precisão. (C) Amostras armazenadas em *eppendorfs* fechados com 1,5 ml de água destilada.

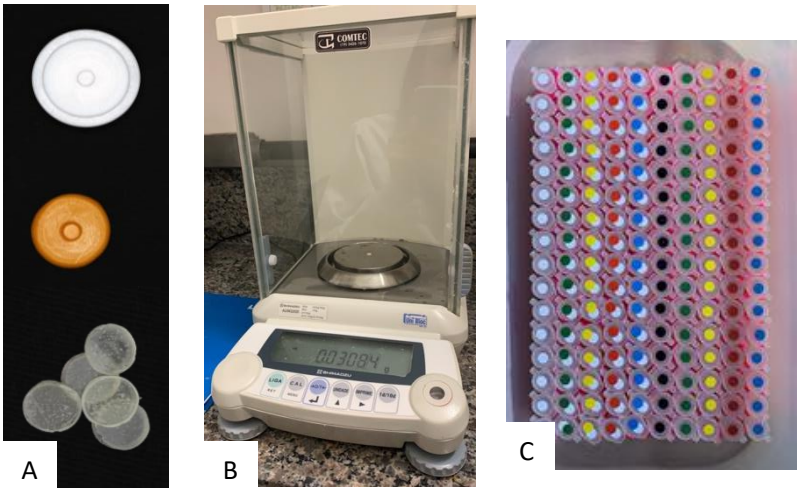

Fonte: Autores

Liberação Iônica

Para esta análise, uma solução com 133mMol/L de cloreto de sódio (NaCl) foi preparada e tamponada com ácido lático 50 mmol/L, até pH 4 (Zixiang et al., 2022). Amostras de infiltrante resinoso de cada grupo (n=3), no tamanho 2x2x12 mm, foram confeccionadas a partir da inserção do material em uma matriz de silicone. Para padronização das amostras, uma matriz de poliéster foi utilizada sobre a matriz de silicone com o infiltrante e, uma fotopolimerização de 40 segundos foi efetuada na superfície e no fundo de cada amostra, totalizando 80 segundos. Depois, cada amostra foi imersa em 17 mL da solução preparada e, as concentrações dos íons de cálcio (Ca), fosfato (P) e flúor (F) foram medidos em dois tempos distintos (14 e 28 dias). Para cada tempo, uma fração de 4 mL da solução foi removida, armazenada em eppendorf e, substituída por uma nova fração. Os eppendorfs com as frações da solução foram mantidos fechados e sob refrigeração durante todo o período. As concentrações dos íons liberados foram quantificadas através de um espectrofotômetro de absorbância (UV-Visible, Thermo Scientific, São Paulo, SP, Brasil) (Figura 4). Para a obtenção das médias, a leitura dos íons de cálcio liberados foi realizada utilizando o método de cálcio arsenazo de ponto único, utilizando valores de absorbância de uma solução padrão, sendo a média aritmética desse padrão derteminada por duplicata. Para os íons de fosfato e flúor foi utilizado o método de curva padrão linear, com duplicata de absorbância para cada ponto do padrão.

Figura 4 – (A) Espectrofotômetro UV-Visible. (B) Cubetas do equipamento preenchidas com amostras.

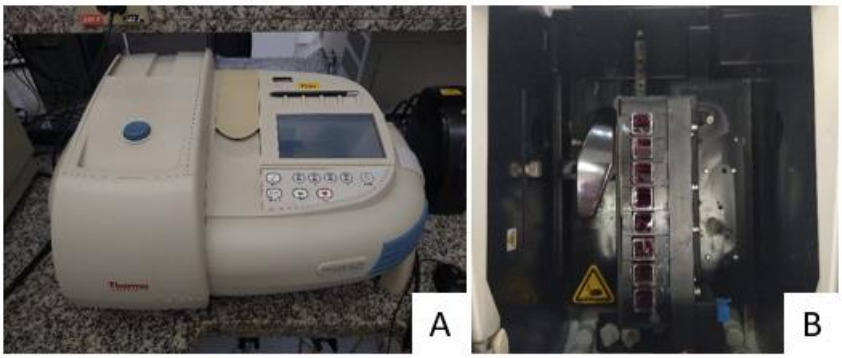

Fonte: Autores

Simulação da lesão cariosa incipiente

Confecção dos corpos de prova

Após aprovação do Comitê de Ética em Pesquisa (nº 654486.22.6.0000.5418), molares humanos hígidos foram selecionados. Os dentes foram limpos com escova de Robinson e pedra pomes, a fim de remover os detritos e, em seguida, foram armazenados em solução de timol à 0,1%. Depois, suas raízes foram seccionadas com auxílio de cortadora metalográfica (Buehler LTD., Lake Bluff, IL, EUA) e dispensadas; na sequência, amostras com dimensões de 5x5x2mm foram obtidos a partir das faces vestibular e palatina dos dentes (Figura 5). Para padronizar as superfícies, os corpos de prova foram levemente planificados em politriz (Arotec S/A Indústria e Comércio, Cotia - SP) com lixas d'água de granulação 600 e 1200 (Buehler) sob refrigeração constante; depois, foram polidos com discos de feltro e solução diamantada (1 µm; Buehler) e, então, armazenados em *eppendorfs* e levados à estufa à 37ºC.

Figura 5 – Corte dos dentes em cortadora metalográfica e amostras em 5x5x2mm.

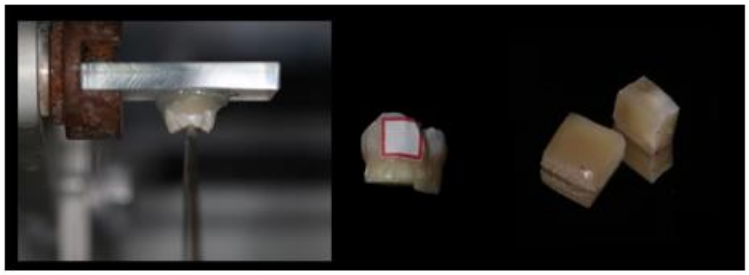

Fonte: Autores

Indução da lesão cariosa incipiente

Após a obtenção das amostras, as médias de microdureza superficial foram obtidas por meio de três leituras em microdureza (HMV-2000; Shimadzu Corporation, Tóquio, Japão), distante 100 µm do centro da superfície, para randomizar as amostras, evitando que os grupos fossem beneficiados ou prejudicados com baixa ou alta microdureza. Após, as amostras foram protegidas com verniz de unha (Colorama®, São Paulo, SP, Brasil) e submetidas à simulação de lesões de cárie incipientes. Para simular a atividade de cárie na cavidade oral, foram utilizadas solução desmineralizante (DES) e solução remineralizante (RE). As amostras foram imersas em 50 ml da solução DES, composta por CH3COOH 0,075 M. CaCl2 1,0 mM. KH2PO4 2,0 mm, pH 4,4, por um período de 6 h; foram então removidas e enxaguadas com água destilada por 10 s. Em seguida, foram colocados em 25 mL da solução RE, composta por KCl 150 mM. CaCl2 1,5 mM. KH2PO4 0,9mM. NH2C(CH2OH)3 20 Mm, pH 7,0, por um período de 18 h. Este protocolo foi realizado durante 7 dias consecutivos e as soluções foram trocadas diariamente (Figura 6) (Al-Obaidi etal., 2019).

Figura 6 – Suporte confecionado para protocolo de indução de lesão de cárie incipiente.

Fonte: Autores

Infiltração dos materiais resinosos

Após a simulação da lesão de cárie incipiente, as amostras foram submetidas à aplicação dos infiltrantes (Figura 7). Assim, tais amostras foram infiltradas, segundo orientações do fabricante do infiltrante resinoso Icon®: condicionamento com ácido hidroclorídrico a 15%, por 2 min. Em seguida, lavagem e secagem, por 30 s cada passo. Aplicação do Icon® Dry (99% etanol) por 30 s e, aplicação dos infiltrantes por 3 min, com remoção dos excessos por uma haste com algodão e, fotopolimerização por 40 s (LED Valo, 1000 mW/cm^2). Seguindo a recomendação do fabricante, a reaplicação do infiltrante por mais 1 min e fotopolimerização por 40 segundos foi realizada em cada grupo. A aplicação dos infiltrantes experimentais foi realizada através de uma seringa descartável de 3 mL, protegida da luz com uma fita isolante preta, e a ponta aplicadora para faces livres que acompanha o kit Icon®.

Figura 7 – (A) Aplicação do Icon® Etch por 2min; (B) Lavagem abundante por 30s com água deionizada; (C) Aplicação do Icon® Dry por 30s; (D) Seringas com os infiltrantes; (E) Fotopolimerização do material por 40s.

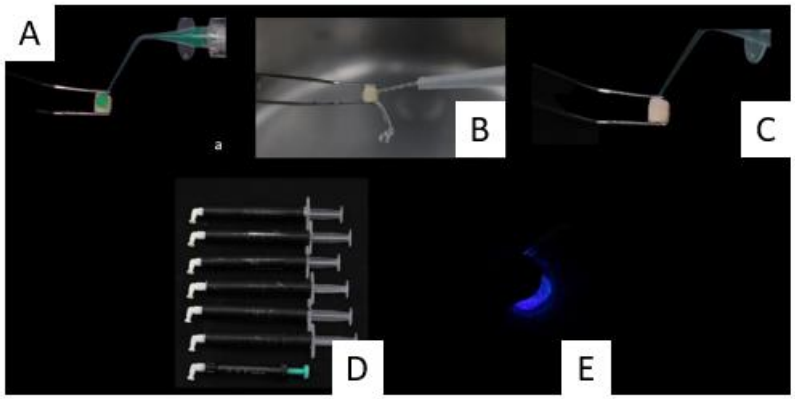

Fonte: Autores

Profundidade de Penetração

Para esta análise, a infiltração resinosa, descrita anteriormente, foi realizada seguindo a técnica de etiquetagem indireta (Figura 8) (Paris et al., 2009). Após a simulação de lesão de cárie incipiente, as amostras de cada grupo (n=5) foram condicionadas com ácido hidroclorídrico a 15% por 2 min; lavadas com jato de água por 30 s e imersas em solução etanólica de rodamina B 0,1% (Sigma Aldrich, Steinheim, Germany) por 12 h (D'Alpino et al., 2006), a fim de preencher os poros acessíveis (pós des-remineralização) com rodamina B, para posterior visualização em microscopia confocal. Decorridas as 12 h, as amostras foram removidas da solução corante, lavadas e secadas por 30 s, cada passo. Na sequência, o Icon® Dry (99% etanol) foi aplicado por 30 s e, os infiltrantes foram aplicados por 3 min com remoção dos excessos por uma haste com algodão e, fotopolimerizados por 40 s (Valo, Ultradent, São Paulo, Brasil). A reaplicação do infiltrante por mais 1 min e fotopolimerização por 40 s foi realizada. Todas as amostras infiltradas foram, posteriormente, cortadas perpendicularmente à superfície da lesão de esmalte, com disco diamantado em cortadora metalográfica e, inicialmente, polidos em politriz com lixas d'água de granulação 600 e 1200 e, posteriormente, à mão livre, sob refrigeração, até que finas fatias com espessura de 100 µm fosse alcançada. Para remover a rodamina B não aderida à estrutura dentária, as fatias foram imersas em peróxido de hidrogênio a 30%, por 12 h. Depois, as amostras foram imersas em solução etanólica de fluoresceína de sódio a 100 µm (NaFl; Sigma Aldrich, St. Louis, EUA), durante 3 min e, lavadas com água destilada por 30 s. Em seguida, foram levadas ao Microscópio Confocal de Varredura a Laser (Leica, TCS SP5; Leica, Heidelberg, Alemanha)

com objetiva de 63x 1.4NA, e imergidas em óleo no modo dual de fluorescência, para obtenção das imagens.

Figura 8 – (A) Aplicação do Icon® Etch por 2min; (B) Lavagem abundante por 30s com água deionizada; (C) Imersão em corante Rodamina B; (D) Aplicação do Icon® Dry por 30s; (E) Aplicação dos infiltrantes sobre a superfície por 3min; (F) Fotopolimerização do material por 40s; (G) Corte transversal da amostra; (H) Fatia da amostra após corte transversal.

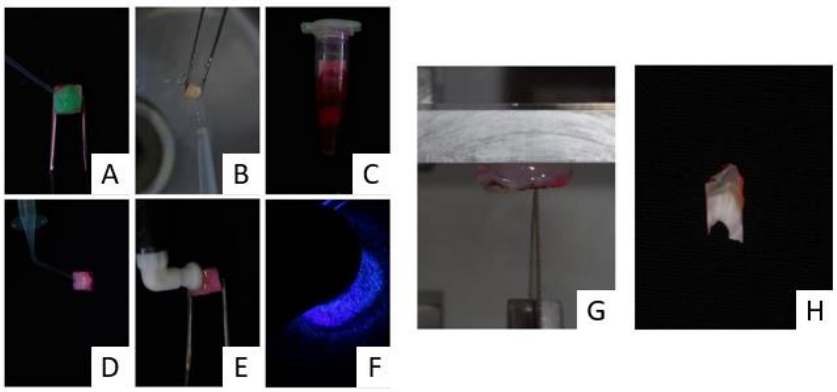

Fonte: Autores

Estabilidade de cor

As amostras de dente humano foram fixadas em pequenas placas de acrílico com cera pegajosa (Figura 9A), ficando à mostra apenas a superfície do esmalte polido; depois, foram imersas em um recipiente com 1,5 L de solução de café, 60 g:1 L (3 Corações®, Sumaré, São Paulo, SP, Brasil) (lote1001078), por um período de 7 dias a 37 °C, com trocas diárias da solução corante (Figura 9B). Para as análises da cor (n=15), as amostras foram removidas das placas de acrílico, enxaguadas com água destilada e, a cor foi avaliada com um espetrofotómetro (Konica Minolta CM-700d, Sensing Americas, Inc., EUA) numa cabine de luz (GTI Newburg, NY, EUA) no modo "luz diária". Um stub que permitia a acomodação da amostra e passagem da luz do espetrofotómetro foi utilizado (Figura 9C). 3 leituras de pontos distintos de cada amostra foram realizadas. A análise da cor foi realizada em três tempos distintos: (T1) esmalte infiltrado, (T2) esmalte manchado e (T3) esmalte polido. Os dados obtidos pelo sistema CIEL*a*b*, que correspondem a L* para a luminosidade, a* para a cromaticidade (vermelho-verde) e b* (azul-amarelo), foram utilizados também na fórmula de variação de cor CIEDE2000 ΔE00 = [(ΔL′ /KLSL) 2 + (ΔC′ / KCSC) 2 + (ΔH′ /KHSH) 2 + RT * (ΔC′/KCSC) * (ΔH′ / KHSH)]1/2, entre os intervalos T1-T2, T2-T3. O índice de brancura dentária (WID) foi calculado usando a fórmula WID =0,511 L*-2,324 a*-1,100b*, seguido da diferença de índice (ΔWID) considerando os intervalos T1-T2, T2-T3. Os limiares de percetibilidade e aceitabilidade seguidos para ΔE00 foram 0,8 para a percetibilidade e 1,8

para a aceitabilidade (Paravina et al., 2019) e, para as diferenças no índice de brancura (ΔWID) foram 0,7 para a percetibilidade e 2,6 para a aceitabilidade (Pérez et al., 2019).

Figura 9 – (A) Amostras fixadas na placa acrílica. (B) Placas acrílicas com amostras fixadas em recipiente para manchamento com café. (C) Stub para acomodação da amostra e espetrofotômetro.

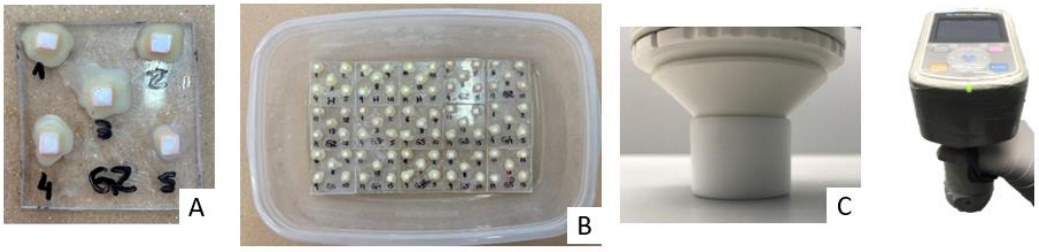

Fonte: Autores

Rugosidade superficial

Após o preparo e infiltração resinosa, descritos anteriormente, as amostras de dente humano foram previamente fixadas (Lysanda, São Paulo, Brasil) em placas acrílicas e levadas ao rugosímetro (Surfcorder, Kosakalab, Toquio, Japão) (Figura 10), configurado com cut off de 0,25 mm e, o comprimento de leitura de 1,25 mm. O raio da ponta de rastreamento era de 2 μm e velocidade de 0,1 mm/s (de Cerqueira et al., 2023). As análises de rugosidade também foram realizadas em três diferentes tempos, sendo (I) esmalte infiltrado, (II) esmalte manchado e (III) esmalte polido. Para cada tempo, três leituras da rugosidade foram feitas e obtidas as médias de cada amostra (n=15).

Figura 10 – Amostra fixada em placa acrílica para leitura no rugosímetro.

Fonte: Autores

ANEXOS

ANEXO 1: Verificação de originalidade e prevenção de plágio

AVALIAÇÃO DE DIFERENTES CONCENTRAÇÕES DO FOSFATO DE CÁLCIO AMORFO E FLUORETO DE ESTANHO SOBRE AS PROPRIEDADES FÍSICAS DE UM RESIN INFILTRANTE RESINOSO EXPERIMENTAL

RELATÓRIO DE ORIGINALIDADE

16%	15%	10%	1%
ÍNDICE DE SEMELHANÇA	FONTES DA INTERNET	PUBLICAÇÕES	DOCUMENTOS DOS ALUNOS

FONTES PRIMÁRIAS

1	www.repositorio.unicamp.br Fonte da Internet	5%
2	opendentistryjournal.com Fonte da Internet	3%
3	www.ncbi.nlm.nih.gov Fonte da Internet	2%
4	repositorio.unicamp.br Fonte da Internet	1%
5	"Full Issue", Operative Dentistry, 2021 Publicação	1%
6	Jade Laísa Gordilio Zago, Gabriela Alves de Cerqueira, Robson de Sousa Ferreira, Flávio Henrique Baggio Aguiar et al. "Evaluation of experimental resin infiltrant containing nanohydroxyapatite on color stability and microhardness in demineralized enamel", Clinical Oral Investigations, 2023 Publicação	1%
7	inis.iaea.org Fonte da Internet	1%
8	www.scielo.br Fonte da Internet	1%

Excluir citações	Em	Excluir correspondências	< 1%
Excluir bibliografia	Em		

ANEXO 2: Certificado de aprovação do Comitê de Ética

UNICAMP - FACULDADE DE ODONTOLOGIA DE PIRACICABA DA UNIVERSIDADE DE CAMPINAS - FOP/UNICAMP

PARECER CONSUBSTANCIADO DO CEP

DADOS DO PROJETO DE PESQUISA

Título da Pesquisa: Avaliação de propriedades físico-químicas e do potencial efeito remineralizante de um infiltrante resinoso experimental contendo Fosfato de Cálcio Amorfo e Fluoreto de Estanho

Pesquisador: GABRIELA ALVES DE CERQUEIRA

Área Temática:

Versão: 4

CAAE: 65448622.6.0000.5418

Instituição Proponente: Faculdade de Odontologia de Piracicaba - Unicamp

Patrocinador Principal: Financiamento Próprio

DADOS DO PARECER

Número do Parecer: 5.851.104

Continuação do Parecer: 5.851.104

Declaração de Manuseio Material Biológico / Biorepositório / Biobanco	Biorrepositorio.pdf	19/12/2022 16:30:27	GABRIELA ALVES DE CERQUEIRA	Aceito
Outros	56Termodoacao.pdf	20/11/2022 12:29:46	GABRIELA ALVES DE CERQUEIRA	Aceito
Outros	autoriz_FTIR.pdf	20/11/2022 12:29:24	GABRIELA ALVES DE CERQUEIRA	Aceito
Outros	autoriz_confocal.pdf	20/11/2022 12:29:02	GABRIELA ALVES DE CERQUEIRA	Aceito
Outros	54altinfra.pdf	20/11/2022 12:28:00	GABRIELA ALVES DE CERQUEIRA	Aceito
Declaração de Pesquisadores	51declarapesquisadores.pdf	20/11/2022 12:25:51	GABRIELA ALVES DE CERQUEIRA	Aceito
Declaração de Instituição e Infraestrutura	52declarainstituicao.pdf	20/11/2022 12:25:31	GABRIELA ALVES DE CERQUEIRA	Aceito
Folha de Rosto	folhaDeRosto.pdf	20/11/2022 12:24:29	GABRIELA ALVES DE CERQUEIRA	Aceito

Situação do Parecer:
Aprovado

Necessita Apreciação da CONEP:
Não

PIRACICABA, 12 de Janeiro de 2023

Assinado por:
jacks jorge junior
(Coordenador(a))

Endereço: Av.Limeira 901 Caixa Postal 52, Prédio Administrativo, Segundo Piso, Setor de Secretarias de Ensino
Bairro: Areião **CEP:** 13.414-903
UF: SP **Município:** PIRACICABA
Telefone: (19)2106-5349 **Fax:** (19)2106-5349 **E-mail:** cep@fop.unicamp.br

ANEXO 3: Submissão do artigo ao periódico